AFGL-TR-76-0275

FG.

STABILIZED LASER GRAVIMETER

Howard C. Merchant
G. Rodney Huggett

Applied Physics Laboratory
University of Washington
Seattle, Washington 98105

1 November 1976

Final Report for Period 1 July 1974 - 31 October 1976

Approved for public release; distribution unlimited

AIR FORCE GEOPHYSICS LABORATORY
AIR FORCE SYSTEMS COMMAND
UNITED STATES AIR FORCE
HANSCOM AFB, MASSACHUSETTS 01731

MIL-STD-847A
31 January 1973

Unclassified

SECURITY CLASSIFICATION OF THIS PAGE (When Data Entered)

REPORT DOCUMENTATION PAGE

READ INSTRUCTIONS BEFORE COMPLETING FORM

1 REPORT NUMBER: AFGL-TR-76-0275	2 GOVT ACCESSION NO
3 RECIPIENT'S CATALOG NUMBER	
4 TITLE (and Subtitle): Stabilized Laser Gravimeter	5 TYPE OF REPORT & PERIOD COVERED: Final Report 1 July 74 - 31 Oct 76
6 PERFORMING ORG. REPORT NUMBER	
7 AUTHOR(s): Howard C. Merchant, G. Rodney Huggett	8 CONTRACT OR GRANT NUMBER(s): F19628-75-C-0042
9 PERFORMING ORGANIZATION NAME AND ADDRESS: Applied Physics Laboratory HN-10, U. Washington, Seattle, WA 98195	10 PROGRAM ELEMENT, PROJECT, TASK AREA & WORK UNIT NUMBERS: 62101F, 8607020
11 CONTROLLING OFFICE NAME AND ADDRESS: Air Force Geophysics Laboratory, Hanscom AFB, Massachusetts 01731, Monitor / James Hammond / LWG	12 REPORT DATE: November 1, 1976
	13 NUMBER OF PAGES: 47
14 MONITORING AGENCY NAME & ADDRESS (if different from Controlling Office)	15 SECURITY CLASS. (of this report): Unclassified
	15a DECLASSIFICATION/DOWNGRADING SCHEDULE

16 DISTRIBUTION STATEMENT (of this Report)

Approved for public release; distribution unlimited.

17 DISTRIBUTION STATEMENT (of the abstract entered in Block 20, if different from Report)

18 SUPPLEMENTARY NOTES

19 KEY WORDS (Continue on reverse side if necessary and identify by block number)

Gravimeter
Laser
Gravity
Geophysical Instrumentation

20 ABSTRACT (Continue on reverse side if necessary and identify by block number)

The development and testing of a stabilized laser gravimeter is discussed. A parametric excitation system that is adaptable to the gravimeter is also described.

next page

cont.

DD FORM 1 JAN 73 1473 EDITION OF 1 NOV 65 IS OBSOLETE

Unclassified

SECURITY CLASSIFICATION OF THIS PAGE (When Data Entered)

Unclassified
SECURITY CLASSIFICATION OF THIS PAGE(When Data Entered)

cont

20., cont.

The design and initial development of the stabilized laser gravimeter system have been previously described in AFCRL-TR-74-0355. In the design a mirror forming one end of a Fabry-Perot optical cavity is mounted on a mechanical suspension system. The suspension consists of a beam, end loaded to obtain the required sensitivity to changes in gravitation. A He-Ne illuminating laser is locked to a fringe of the Fabry-Perot cavity. A He-Ne laser stabilized by locking to a vibration-rotation absorption line of a methane cell is used as a reference. The output of the system is a beat frequency between the two lasers proportional to the gravity change.

The proposed parametric excitation system applies a periodic end load in addition to the static load on the beam suspension system. It has been shown theoretically and experimentally that significant (order of magnitude) gains in sensitivity can be realized by parametric excitation.

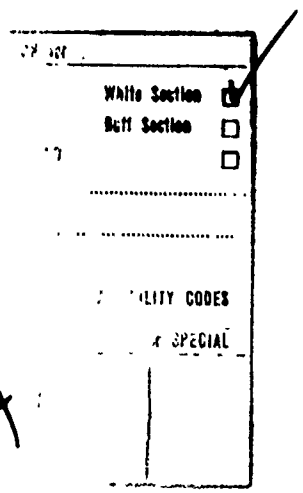

Unclassified
SECURITY CLASSIFICATION OF THIS PAGE(When Data Entered)

CONTENTS

LIST OF FIGURES

ACKNOWLEDGMENTS

The following people contributed to the development of the system described here and/or to the text of this report: Mr. Karlheinz Eisinger and Mr. George Bondor.

The many helpful discussions with Dr. James A. Hammond are also acknowledged.

RELATED DOCUMENTS AND PUBLICATIONS

Quarterly reports for contract F19628-73-C-0203:

Laser Stabilized Gravimeter #1
(May 1, 1973 to July 31, 1973)

Laser Stabilized Gravimeter #2
(August 1, 1973 to October 31, 1973)

Laser Stabilized Gravimeter #3
(November 1, 1973 to January 31, 1974)

Laser Stabilized Gravimeter #4
(February 1, 1974 to April 30, 1974)

H.C. Merchant, E.N. Hernandez, and N.D. McMullen, "Stabilized Laser Gravimeter," Proceedings of the 20th International Instrumentations Symposium, Albuquerque, New Mexico, May 1974.

N.D. McMullen, "Methane Absorption Stabilized Laser Gravimeter: Design of an Ultra-Sensitive Fabry-Perot Interferometer Accelerometer," M.S. Thesis, Mechanical Engineering, University of Washington, 1974.

H.C. Merchant, "Stabilized Laser Gravimeter," AFCRL-TR-74-0355, July 1974.

Quarterly reports for contract F19628-75-C-0042:

Laser Stabilized Gravimeter #2
(October 1, 1974 to December 31, 1974)

Laser Stabilized Gravimeter #3
(January 1, 1975 to March 31, 1975)

Laser Stabilized Gravimeter #4
(April 1, 1975 to June 30, 1975)

Laser Stabilized Gravimeter #5
(July 1, 1975 to September 30, 1975)

Laser Stabilized Gravimeter #6
(October 1, 1975 to December 31, 1975)

Laser Stabilized Gravimeter #7
(January 1, 1976 to March 31, 1976)

George S. Bondor, Jr., "Calibration and Error Analysis of a Stabilized Laser Gravimeter," M.S. Thesis, Mechanical Engineering, University of Washington (in preparation), 1977.

Karlheinz Eisinger, "Parametric Excitation of a Clamped Beam," Ph.D. Thesis, Mechanical Engineering, University of Washington (in preparation), 1977.

INTRODUCTION

The basic instrument used in the tests discussed in this report has previously been described by Merchant [1,2].

The instrument is a static gravimeter as opposed to a pendulum or free-fall apparatus. The gravimeter consists of a mass elastically suspended so that changes in gravitation (or acceleration) will result in a detectable relative motion of the seismic mass. The mass consists of a mirror and holder, and the detection system uses two lasers. The mirror is the retro-reflector of a high-finesse Fabry-Perot cavity, an optical resonator with very narrow transmission fringes. The wavelength of an external He-Ne illuminating laser is locked to changes in the cavity length by following a single fringe. The reference frequency is provided by a second He-Ne laser which is stabilized by inserting a methane cell in the cavity, and locking the laser frequency to the molecular absorption line of methane. The output is the beat frequency between the stabilized reference laser and the cavity-locked laser. The optical system is an adaptation of the techniques used by Levine and Hall [3] for a strainmeter.

The microgal resolution needed for a useful gravimeter requires a very high resolution laser and a very low natural frequency (soft) mechanical suspension system. To obtain the necessary mechanical sensitivity, a suspension system consisting of an endloaded beam was used. Theoretically, the natural frequency and spring stiffness of the system approach zero as the end load approaches the buckling load for the beam system [4,5].

A vacuum system was constructed to enclose the Fabry-Perot sensing cavity and the system was installed at a University of Washington Geophysics test site at Tumwater, Washington.

---

1. H.C. Merchant, "Stabilized Laser Gravimeter," AFCRL-TR-74-0355, Air Force Cambridge Research Laboratories, Hanscom Air Force Base, Massachusetts, July 1974.

2. H.C. Merchant, E.M. Hernandez and N.D. McMullen, "Stabilized Laser Gravimeter," Proceedings of the 20th International Instrumentations Symposium, Albuquerque, New Mexico, May 1974.

3. J. Levine and J.L. Hall, "Design and Operation of a Methane Absorption Stabilized Laser Strainmeter," Journal of Geophysical Research, Vol. 77, No. 14 (May 1972) pp. 2595-2609.

4. L. Meirovitch, Analytical Methods in Vibrations, Macmillan, New York (1967).

5. H. Lurie, "Lateral Vibrations as Related to Structural Stability," Journal of Applied Physics, June 1952, pp. 195-204.

The use of parametric excitation to increase the sensitivity of the system has been demonstrated theoretically and on a laboratory model. The parametric excitation is introduced as a periodic component superimposed on the static end load of the beam support system. The sensing mass and mirror in the Fabry-Perot cavity are carried on the parametrically excited support beam, resulting in an amplified mirror deflection.

EXPERIMENTAL SETUP, FIELD TESTS

The components of the gravimeter are shown schematically in Figure 1, and their function is identified. Figure 2 shows the beam support system and the center mass containing a mirror, which is identified in Figure 1 as the accelerometer. Figure 3 shows the complete Fabry-Perot cavity without the vacuum chamber. The beam and detector mass are visible at the bottom in the endloading housing and the He-Ne illuminating laser for the cavity is visible at the right. Figure 4 shows the vacuum housing for the cavity. The laser beam enters through a quartz window. Figure 5 shows the Fabry-Perot cavity enclosed in its vacuum housing, as installed at the test site at Tumwater, Washington. The He-Ne illuminating laser is visible at the center and the methane-stabilized reference laser is in the foreground. The beat frequency detector is visible at the left. The details of the construction and operation of the system have been reported previously.

The field tests were intended to obtain earth tides for comparison with predicted values over a time period long enough to check the stability and sensitivity of the system. However, due primarily to equipment reliability, the maximum periods during which data could be obtained were hours rather than days [6].

Problems encountered in the field tests were: degradation in laser outputs as a function of time; multiple resonances in the Fabry-Perot cavity, and multiple-cavity interaction between the Fabry-Perot cavity and the He-Ne illuminating laser cavity; degradation of the optical isolation system with time (apparently due to moisture sensitivity); and electronic failures in the servo system and the long-path (Fabry-Perot) detector system.

The laser degradation was alleviated by periodic laser realignment. The multiple resonance and cavity interaction were eliminated by changes in the cavity configuration and replacement of the optical isolation system with one with a higher transmission coefficient. This higher quality system also eliminated the initial problem with the optical isolation system. The servo system was repaired before the end of the contract period, but components to rebuild the long-path detector could not be obtained in the contract period.

---

6. Laser Stabilized Gravimeter Quarterly Report, Nos. 3 through 7, Contract F19628-75-C-0042 (1975-76).

Therefore, as stated before, operation of the system was confined to a few hours. However, this did allow the evaluation of the operating parameters [1] and error sources as discussed in the following section.

ERROR ANALYSIS AND TESTS

The following sources of error were examined:

a) The variation in vacuum in the Fabry-Perot cavity.

b) The variation in temperature in the Fabry-Perot cavity.

c) Creep in the structural materials.

d) Gravity noise due to tilt.

e) Background noise due to personnel movements and local vehicular traffic.

The vacuum chamber surrounding the Fabry-Perot cavity was not constructed to obtain a high vacuum but rather to ensure a stable condition. The effect of a change in pressure is a change in the speed of light and hence the cavity resonance frequency. This frequency change is reflected in an apparent gravity error (Δg) as follows:

$$\Delta g = (\Delta L)\, \omega_n^2 \quad , \tag{1}$$

where

$$\Delta L = -\frac{\Delta f}{f} L$$

$$\Delta f = f - f_\Delta$$

$$f = \frac{V}{2L}$$

$$f_\Delta = \frac{V_\Delta}{2L} \, ,$$

and

Δg = gravity error

ω_n = natural frequency of the sensing mass (and mirror)

ΔL = apparent cavity length change (deflection of sensing mass)

L = original cavity length

f = original cavity frequency

Δf = frequency change in cavity

f_Δ = perturbed cavity frequency

V = velocity of light at the original condition

V_Δ = velocity of light at the perturbed condition.

Variation of temperature can affect the system in two ways. The first is through a change in the speed of light and the second through thermal deformation of the structure. The first effect is handled theoretically in the same manner as the pressure effect and hence they will be discussed together.

There have been several investigations, both theoretical and empirical, to determine the relationship between the index of refraction (and hence the speed of light) and the parameters that affect it [7, 8, 9, 10]. The most recent is by Owens [10]. His results were used to predict the sensitivity of the gravimeter to pressure changes and the aspect of temperature change that affects the index of refraction.

The velocity of light in a medium is related to the index of refraction by

$$V = \frac{C}{n} ,$$

where

C = the velocity in a vacuum
n = the index of refraction.

Owens' results are:

---

7. H. Barrell and J.E. Sears, "The Refraction and Dispersion of Air for the Visible Spectrum," Philosophical Transactions of the Royal Society of London, Series 4, Vol. 238 (1940) pp. 1-64.

8. Elden Bengt, "The Dispersion of Standard Air," Journal of the Optical Society of America, Vol. 43, No. 5 (May 1, 1953), pp. 339-344.

9. Elden Bengt, "The Refractive Index of Air," Metrologia, Vol. 2, No. 2 (April 1966) pp. 71-80.

10. James C. Owens, "Optical Refractive Index of Air: Dependence on Pressure, Temperature and Composition," Applied Optics, Vol. 6, No. 1 (January 1967) pp. 51-59.

$$(n-1) = \left[S_1 + \frac{S_2}{S_3 - \sigma^2} + \frac{S_4}{S_5 - \sigma^2}\right] D_s$$

$$+ \left[\omega_1 + \omega_2\sigma^2 + \omega_3\sigma^4 + \omega_4\sigma^6\right] D_\omega \,, \qquad (2)$$

where

$$D_s = \frac{P_s}{T}\left[1 + P_s\left(S_6 + \frac{S_7}{T} + \frac{S_8}{T^2}\right)\right]$$

$$D_\omega = \frac{P_\omega}{T}\left[1 + P_\omega\left(1 + \omega_5 P_\omega\right)\left(\omega_6 + \frac{\omega_7}{T} + \frac{\omega_8}{T^2} + \frac{\omega_9}{T^3}\right)\right]$$

$\sigma = \frac{1}{\lambda}$

λ = wavelength (angstroms)

P_s = partial pressure of air (millibars)

P_ω = partial pressure of water vapor (millibars)

T = temperature (degrees Kelvin)

and

i	S_i	ω_i
1	2371.34×10^{-8}	6487.31×10^{-8}
2	683939.7×10^{-8}	58.058×10^{-8}
3	130	-0.7115×10^{-8}
4	4547.3×10^{-8}	0.08851×10^{-8}
5	38.9	3.7×10^{-4}
6	57.9×10^{-8}	-2.37321×10^{-3}
7	-9.325×10^{-4}	2.23366
8	0.25844	-710.792
9	-	7.75141×10^{-4}

The formula assumed atmospheric air to be made up of dry carbon dioxide free air, water vapor, and carbon dioxide. The partial pressures of air and water vapor required can be determined by assuming ideal gas behavior at low pressure.

The assumed reference conditions to determine the effects of pressure and temperature changes were

$T = 300°K$

$P = 1$ mm Hg

Relative Humidity = 50%

$\lambda = 3.39\ \mu = 33{,}900\ \text{Å}$

The results of applying the foregoing equation are:

Pressure

$\Delta g = 14.126$ milligals/mm Hg

Temperature

$\Delta g = 16.7$ microgals/degree K.

The experimental method used to check the pressure effects on the system was to evacuate the system, shut off the vacuum system, and introduce a controlled leak while monitoring the frequency of the Fabry-Perot cavity as a function of vacuum. The test times were short compared to thermal delay times and earth tide periods. The pressure changes selected were several orders of magnitude (2 mm Hg or more) beyond the system's operational fluctuations, to obtain a large error output. The predicted values for Δg/mm Hg ranged from 30% to 40% below the values obtained during three pressure tests. Therefore, the foregoing calculations for pressure error provide a conservative estimate of the pressure effect.

To investigate the thermal effects on the index of refraction, the system was operated with the vacuum system on and the aluminum vacuum housing heated at a series of locations. The gravimeter output was monitored during the heating period and for 45 minutes afterward. Temperatures were measured with thermocouples attached to the vertical quartz support rods (Figure 3, longest rods), to the quartz rods supporting the mechanical sensing system (Figure 3, short rods), and to the steel spacers (Figure 3, on top of short quartz rods), and with two thermocouples suspended in the cavity next to the laser beam path.

The other aspect of the thermal effect on the gravimeter is the change in cavity length due to thermal expansion. The support for the Fabry-Perot cavity is designed so that the sensor is on re-entry rods of quartz and spacers of steel (Figure 3). The support members are dimensioned so that the thermal expansion of the re-entry supports cancels the expansion of the lateral supports [1, 11]. This, of course, is the case when there are no thermal gradients between the support elements.

---

11. N.D. McMullen, "Methane Absorption Stabilized Laser Gravimeter: Design of an Ultra-Sensitivity Fabry-Perot Interferometer Accelerometer," M.S. Thesis, Mechanical Engineering, University of Washington, 1974.

In the tests performed, thermal gradients were developed in the supports that resulted in cavity length changes that produced errors several orders of magnitude greater than those that would be predicted from the temperature change (1°K) obtained in the partial vacuum. Therefore only qualitative statements can be made about the relative magnitude of the three sources of error--thermal expansion, pressure changes, and direct temperature changes in the cavity. The results indicate that the direct temperature changes will cause errors that are orders of magnitude smaller than the pressure fluctuations. Therefore the most important thermal concern is maintaining a uniform temperature in the gravimeter structure.

Creep is defined as slow deformation of solid materials over extended periods of time. Temperature and stress in the material are parameters in the creep process. The element in the system most sensitive to creep is the support beam since the material is steel and it is the most highly stressed. For the creep to be important, temperatures on the order of one-half the melting temperature and stresses that are a significant percentage of the yield stress must occur [12]. The maximum end load required to obtain the desired natural frequency of the sensing beam support system (2.5 Hz) is 14.2×10^6 dynes with a resulting stress of 2.8×10^8 dynes/cm^2 [13]. The yield strength for the beam material is 1.38×10^{10} dynes/cm^2. The operating temperature will be less than 35°C while one-half the melting temperature is approximately 750°C. Therefore, no experimental creep tests were performed.

The effect of tilt at the measuring site on the gravimeter output was examined by introducing a large tilt at the base of the instrument and scaling the effect to geophysical levels. The entire gravimeter system was mounted on a granite slab, the edge of which is visible in the foregound of Figure 5. A tilt was introduced by raising the edge of the slab with a hydraulic jack while monitoring the slab motion with dial indicators supported on a frame over the slab. When the results were scaled to actual geophysical tilt levels of 10^{-9} radian, the tilt error was on the order of 1 μgal and therefore within the accuracy of the gravimeter.

A discussion of the linear vibration analysis of the sensing system is given by McMullen [11] and Bonder [13]. A discussion of the nonlinear aspects by Eisinger [14] is summarized in the following section. The

---

12. L. Finnie and W.R. Heller, Creep of Engineering Materials, McGraw-Hill, New York, New York 1959.

13. G. Bondor, "Calibration and Error Analysis of a Stabilized Laser Gravimeter," M.S. Thesis, Mechanical Engineering, University of Washington (in preparation), 1977.

14. K. Eisinger, "Parametric Excitation of a Clamped Beam," Ph.D. Thesis, Mechanical Engineering, Univeristy of Washington (in preparation), 1977.

purpose of the tests was to identify operational problems empirically. Three types of inputs were used: vehicular traffic immediately adjacent to the test site structure on the access road; personnel movement in the test site; and impacts adjacent to the test slab. The impact tests were drop tests with metal-to-metal impact to provide a higher frequency input spectrum than obtained by foot falls. An impact of 1.9 joules (newton meters) was produced on the building floor just adjacent to the isolation gap between the pier and the building floor, at 2 meters from the gap, and about 3 meters from the gravimeter on the rock outcropping to which the pier is attached. The results indicate that the disturbances caused a gravimeter output up to 85 milligals, which is far above the microgal sensitivity required. However, the purpose of the gravimeter is to measure phenomena with periods of hours, so such disturbances only create spikes of noise in the data which can be filtered at the time of recording or during data analysis. The important consideration is the ability of the system to maintain laser lock and provide continuous data. This was accomplished in all the tests.

PARAMETRIC EXCITATION

The gravimeter mechanical sensor and suspension system in Figure 2 is shown schematically in Figure 6. In the present configuration the end load [P(t)] is a constant, selected to obtain the desired frequency and hence sensitivity. By allowing the end load to be a time-varying parameter with a specific frequency and mean load, it is possible to obtain increased displacement of the sensing mass to a given change in gravity and hence an increased gravimeter sensitivity. This phenomenon is called parametric excitation or parametric amplification and has been known for many years. The phenomenon was observed by Faraday (1831), Melde (1859) and Rayleigh (1883). Supporting theory was developed initially by Mathieu (1868) and Hill (1886). It was later applied in electrical circuits. The particular configuration of an endloaded beam without parametric excitation has been considered in a great many papers up to the present day. A detailed bibliography on parametric excitation and related phenomena is given in Appendix A. A series of papers by Rodgers [15, 16, 17, 18] presents the development of an electromechanical parametric amplifier for use in a seismometer.

---

15. P.W. Rodgers, "Parametric Phenomena as Applied to Vibration Isolation and Mechanical Amplifiers," Journ. Sound and Vib., Vol. 5, No. 3 (1967) p. 486.

16. P.W. Rodgers, "Sub-Resonant Response of a Mechanical System, Parametrically Excited at the Resonant Frequency," Nature, August 21, 1965, p. 853.

17. P.W. Rodgers, "A Spring with Time-Variable Stiffness," Journ. of Acoust. Soc. of Am., Vol. 39, No. 4 (1966) p. 749.

18. P.W. Rodgers, "A Phase Sensitive Parametric Seismometer," Bull. of Seismological Soc. of Am., Vol. 56, No. 4 (1966) p. 949.

The analytical and experimental models were selected to be compatible with the existing gravimeter configuration. A schematic view of the experimental setup is shown in Figure 7, and a photograph in Figure 8. A beam of the same dimensions as the gravimeter sensing element with a center mass (including the mass of the accelerometer) equal to that of the gravimeter mirror holder mass is visible in the fixture. The static end load is provided by the lever system visible at either end. The dynamic end load is provided by piezoelectric elements, shown in Figure 9 as a cylinder at the center of the figure (the final configuration was a cylindrical stack of ceramic disks for greater output). The flexure support to maintain the beam boundary conditions while allowing the end load to be applied is shown at the left. The complete experimental setup is shown in Figure 10. The parametric system is supported on shock cords and driven by an electromagnetic exciter through a direct current amplifier.

The first experiments repeated Rodgers' tests to check out the effect in the primary parametric amplification mode for the present configuration. The results are shown in Figure 11. Trace A is the beam response to an endload signal at twice the beam's fundamental frequency. The low level response is due to imperfections in the beam and its alignment in a gravity field. Trace B is the beam response to a low level base input (perpendicular to the plane of the beam) with no variation in the end load. Trace C is the result of the same base input and periodic end loads together, and demonstrates parametric excitation. In the present application, the system must exhibit parametric amplification for an input signal with a frequency much less than the natural frequency of the sensing element which will be identified here as secondary parametric excitation. The variables that can be controlled are the magnitude of the static end load and the frequency and magnitude of the dynamic end load. Sinusoidal end loads were used in the experimental and theoretical studies. The following matrix distinguishes between primary and secondary parametric excitation.

	Dynamic endload		Base motion $v^{(g)}$		Phase
	Frequency	Amplitude	Frequency	Amplitude	
Primary parametric amplification (Melde's effect)	$2\ f_n$	any	$\approx f_n$	any	$\approx 0°$
Secondary parametric amplification	$\leq f_n$	$F(\omega^2)$	$<< f_n$	any	any

f_n = system natural frequency; ω = endload frequency

If the following assumptions are made about the system shown in Figure 6,

a) Constant density, area, modulus, and moment of inertia along the beam

b) Small deflections

c) Linear viscous damping for transverse motion (β)

d) The same input motion (acceleration) at both support points ($v_{tt}^{(g)}$)

e) End load $P(t) = P_o + P_1 \cos \omega t$,

the resulting equations of motion are [14]:

$$v_{tt} + \beta v_t + \frac{kAG}{\mu}\left(\phi_x - v_{xx}\right) - \frac{EA}{\mu}\left(u_x v_x\right)_x - \frac{EA}{2\mu}\left(v_x^3\right)_x = -v_{tt}^{(g)} \quad (3)$$

with boundary conditions: $v(\ell,t) = v(-\ell,t) = 0$

$$\phi_{tt} - \frac{EI}{J}\phi_{xx} + \frac{kAG}{J}\left(\phi - v_x\right) = 0 \quad (4)$$

with boundary conditions: $\phi(\ell,t) = \phi(-\ell,t) = 0$

and

$$u_{tt} - \frac{EA}{\mu}u_{xx} - \frac{EA}{4\mu}\left(v_x^2\right)_x = 0 \quad (5)$$

with boundary conditions: $u_x(\ell,t) + \frac{v_x^2(\ell,t)}{2}$

$$= -\frac{P_o}{EA} - \frac{P_1}{EA}\cos \omega t$$

$$u(o,t) = 0,$$

where u,v, and ϕ are the coordinates shown in Figure 6, and

μ = beam mass per unit of length
β = damping coefficient
A = area
E = Young's modulus
G = shear modulus
I = area moment of inertia
J = polar moment of inertia
k = cross section shape factor
ℓ = beam length/2
ω = end load frequency

A Galerkin analysis follows in which a solution in the form of a series of comparison functions satisfying the boundary conditions is assumed. For this analysis it is convenient to combine the three equations. For this to be accomplished, equation (5) must be solved and the value substituted in (3). Closed form solution of equation (5) is possible if the nonlinear coupling term $(v_x/2)^2$ is small when compared to u_x. This depends upon the magnitude of the input, $v_{tt}^{(g)}$, and/or P_o and P_1. For the conditions shown below that are required for parametric excitation in the gravimeter, the nonlinear term may be neglected [14]. The result is:

$$
\begin{aligned}
&EI\, v_{xxxx} - \frac{EI}{kAG} P_1 \chi\lambda^4 \sin\lambda x \cos\omega t\, v_x \\
&\quad + 3\frac{EI}{kAG} P_1 \chi\lambda^3 \cos\lambda x \cos\omega t\, v_{xx} \\
&\quad + 3\frac{EI}{kAG} P_1 \chi\lambda^2 \sin\lambda x \cos\omega t\, v_{xxx} - \frac{EI}{kAG} P_o v_{xxxx} \\
&\quad - \frac{EI}{kAG} P_1 \chi\lambda \cos\lambda x \cos\omega t\, v_{xxxx} \\
&\quad + 3\frac{E^2I}{kG} v_{xx}^3 + 9\frac{E^2I}{kG} v_x v_{xx} v_{xxx} + \frac{3}{2}\frac{E^2I}{kG} v_x^2 v_{xxxx} \\
&\quad - \beta\frac{EI}{kAG} v_{txx} - \mu(x)\frac{EI}{kAG} v_{ttxx} - P_1 \chi\lambda^2 \sin\lambda x \cos\omega t\, v_x \\
&\quad + P_o v_{xx} + P_1 \chi\lambda \cos\lambda x \cos\omega t\, v_{xx} - \frac{3}{2} EA\, v_x^2 v_{xx} \\
&\quad + \beta v_t + \mu(x)\, v_{tt} - J v_{xxtt} + \frac{J}{kAG} P_1 \omega^2 \chi\lambda^2 \sin\lambda x \cos\omega t\, v_x \\
&\quad + 2\frac{J}{kAG} P_1 \omega\chi\lambda^2 \sin\lambda x \sin\omega t\, v_{xt} - \frac{J}{kAG} P_1 \chi\lambda^2 \sin\lambda x \cos\omega t\, v_{xtt} \\
&\quad - \frac{J}{kAG} P_1 \omega^2 \chi\lambda \cos\lambda x \cos\omega t\, v_{xx} - 2\frac{J}{kAG} P_1 \omega\chi\lambda \cos\lambda x \sin\omega t\, v_{xxt} \\
&\quad + \frac{J}{kAG} P_o v_{xxtt} + \frac{J}{kAG} P_1 \chi\lambda \cos\lambda x \cos\omega t\, v_{xxtt} - 3\frac{JE}{kG} v_{xt}^2 v_{xx} \\
&\quad - 3\frac{JE}{kG} v_x v_{xx} v_{xtt} - 6\frac{JE}{kG} v_x v_{xt} v_{xxt} - \frac{3}{2}\frac{JE}{kG} v_x^2 v_{xxtt} + \beta\frac{J}{kAG} v_{ttt} \\
&\quad + \frac{\mu(x)J}{kAG} v_{tttt} = -\mu(x)\, v_{tt}^{(g)} - \frac{\mu(x)J}{kAG} v_{tttt}^{(g)}\,, \qquad (6)
\end{aligned}
$$

subject to the boundary conditions (homogeneous equation):

$$v(\ell,t) = v(-\ell,t) = 0$$

$$v_x(\ell,t) = \phi(\ell,t) + \gamma(\ell,t) = 0$$

$$v_x(-\ell,t) = \phi(-\ell,t) + \gamma(-\ell,t) = 0 ,$$

where the variables are as defined previously and

$$\lambda = \left(\frac{\mu\omega^2}{EA}\right)^{1/2}$$

and

$$\chi = \frac{1}{\left(\frac{\mu\omega^2}{EA}\right)^{1/2} \cos \lambda\ell} .$$

The system's response of interest is the fundamental (first symmetric) mode. Therefore, we use only one term in the approximate solution, with a comparison function approximating the first mode of the linearized system (ϕ_1). The assumed solution is:

$$v(x,t) = \phi_1(x)q(t) ,$$

where q(t) describes the motion of the beam center. This assumption results in a fourth-order equation in the variable q. For a slender beam of the gravimeter configuration and for a low excitation (base motion) frequency, the equation can be approximated by a damped, forced, nonlinear Mathieu equation,

$$\tilde{\alpha}_{21}\ddot{q} + \tilde{\alpha}_{11}\dot{q} + (\tilde{\alpha}_{01} + \tilde{\alpha}_{02} \cos \omega t)\, q + \tilde{\beta}_o q^3 + \tilde{\beta}_1 \ddot{q} q^2 + 2\tilde{\beta}_1 \dot{q}^2 q$$

$$= -\tilde{\gamma}_1 v_{tt}^{(g)} . \qquad (7)$$

The equation was numerically integrated and a linearized version of the equation was analyzed for conditions consistent with the gravimeter. The results were within a percent of each other. The linearized equation, which was used to prepare the stability and amplification plots shown in Figures 13-15, is:

$$\frac{d^2q}{dt^2} + 2\zeta\alpha\frac{dq}{dt} + (\alpha^2 - \gamma_1 \cos \omega t)\, q = -\gamma_2 \tilde{A} \sin \omega t , \qquad (8)$$

where

$$\alpha^2 = \tilde{\alpha}_{01}/\tilde{\alpha}_{21}$$

$$\gamma_1 = -\tilde{\alpha}_{02}/\tilde{\alpha}_{21} \ , \ \tilde{A} = \text{acc. amplitude in m/sec}^2$$

$$\frac{\tilde{\alpha}_{11}}{\tilde{\alpha}_{21}} = 2\zeta\sqrt{\frac{\tilde{\alpha}_{01}}{\tilde{\alpha}_{21}}}$$

$$\tilde{\alpha}_{21} = 3\mu_o + 4\frac{m}{\ell} + \frac{EI}{kAG}\left(\frac{\pi}{\ell}\right)^2\left[\mu_o + 2m\frac{1}{\ell}\right]$$

$$-J\left(\frac{\pi}{\ell}\right)^2 - \frac{J}{kAG}P_o\left(\frac{\pi}{\ell}\right)^2$$

$$\tilde{\alpha}_{12} = \frac{7}{2\pi}\frac{J}{kAG}P_1\,\omega\chi\ell\,\lambda^4 + 2\frac{J}{kAG}P_1\,\omega\chi\left(\frac{\pi}{\ell}\right)^2$$

$$\tilde{\alpha}_{01} = EI\left(\frac{\pi}{\ell}\right)^4 - P_o\left[\left(\frac{\pi}{\ell}\right)^2 + \frac{EI}{kAG}\left(\frac{\pi}{\ell}\right)^4\right]$$

$$\tilde{\alpha}_{02} = P_1\left[-3\frac{EI}{kAG}\chi\lambda^3\left(\frac{\pi}{\ell}\right)^2 + \frac{7}{4\pi}\frac{EI}{kAG}\chi\lambda^6\,\ell + \frac{21}{4}\,\pi\frac{EI}{kAG}\lambda^4\chi\frac{1}{\ell}\right.$$

$$- \frac{EI}{kAG}\chi\lambda\left(\frac{\pi}{\ell}\right)^4 + \frac{7}{4\pi}\chi\beta\lambda^4 - \chi\lambda\left(\frac{\pi}{\ell}\right)^2$$

$$\left. - \frac{7}{4\pi}\frac{J}{kAG}\omega^2\chi\ell\lambda^4 + \frac{J}{kAG}\omega^2\chi\lambda\left(\frac{\pi}{\ell}\right)^2\right] .$$

This equation can be transformed to a standard form,

$$\frac{d^2y}{dz^2} + (a - 2\bar{q}\cos 2z)\,y = F(z) \qquad (9)$$

where

$$F(z) = B\sin\Omega z$$

$$q(z) = e^{-\kappa z}\,y(z) \ , \ \omega t = 2z$$

$$a = 4\frac{\alpha^2}{\omega^2}\left(1 - \zeta^2\right) = \bar{a} - \kappa^2$$

$$\bar{q} = 2\frac{\gamma_1}{\omega^2}$$

$$B = -4\frac{\gamma_2\tilde{A}}{\omega^2}e^{\kappa z}$$

$$\Omega = 2\frac{\delta}{\omega}$$

$$\kappa = 2\zeta\frac{\alpha}{\omega} \quad .$$

The solution for the homogeneous equation is given in terms of Mathieu functions (integral and fractional order). A stability plot for the equation as a function of the parameters a and $\bar{q}$ is shown in Figure 12. The solutions of the forced equation show that the desired response at the frequency of the input is modulated by other, multiple (higher) frequency components. An analysis of the solution in the stable regions of Figure 12 shows that both parametric amplification and parametric attenuation can occur. Figures 13 and 14 show the amplification (or attenuation) curves for the first three regions. Figure 15 shows the effect of damping in regions 2 and 3. Figure 16 gives the computer calculated response for parameters in region 3 (amplification) showing the modulated signal. Figure 17 shows the low-pass filtered signal.

The above data can be used to select the coefficients of the Mathieu equation that will result in amplified responses that correspond to the stable region in Figure 12. A more useful presentation for design purposes, however, is given in Figures 18 and 19.

If a constant value for the parameter $\bar{q}$ in Figure 12 is considered, it is possible to plot the points of intersection with the characteristic curves (a_i and b_i) in Figure 12 in terms of the static end load (P_o), the total dynamic endload magnitude ($P_o \pm P_1$), the endload frequency (ω), and the transverse frequency of the beam (α). One example of such a plot is shown for $q = 1$ in Figure 18, which gives the static end load (normalized by the critical buckling load, P_{cr}) as a function of the endload frequency (normalized by the transverse undamped natural frequency of the nonendloaded beam, α_o) Figure 19 is another example for $q = 1$ that plots the magnitude of the dynamic end load as a function of the transverse beam frequency. A set of curves (with a range of $\bar{q}$ values) would allow the selection of the static end load, dynamic end load, and endload frequency to attain a desired point in the stability and amplification regions shown in Figures 12 through 14.

The results of one of the experiments conducted to verify the foregoing theory of secondary parametric amplification are shown in Figure 20. The system parameters are shown on the figure; the experimental setup was the same as shown in Figures 7-10. The high frequency modulation is also apparent in the case of secondary amplification.

CONCLUSIONS AND RECOMMENDATIONS

The approach taken to develop a gravimeter using a mechanical sensor in the form of an endloaded beam and a stabilized laser sensing system still holds promise. No experimental or theoretical reasons have been identified that would prevent the operation of such a gravimeter. However, it has not been possible within the contract period to operate the instrument at its theoretical sensitivity for a period of time long enough to obtain earth tides. The potential of using parametric excitation to further increase the sensitivity of this gravimeter or for a similar application has also been demonstrated theoretically and experimentally.

It is recommended that a system using visible red light (6328 Å) and an iodine rather than a methane absorption line be constructed. This would produce the following benefits:

a) A decrease in cavity size, with a corresponding decrease in potential sources of errors

b) A direct current rather than RF-excited system, which would alleviate noise problems associated with the detection system in the present configuration

c) The direct alignment of the system with the operating red light beam rather than with an auxiliary laser system, which would allow more accurate initial alignment and routine monitoring of the system.

It is not recommended that parametric excitation of a gravimeter system be carried beyond its present state of development until either the present methane-stabilized system or an iodine-stabilized system has successfully demonstrated its ability to detect earth tides.

REFERENCES

1. H.C. Merchant, "Stabilized Laser Gravimeter," AFCRL-TR-74-0355, Air Force Cambridge Research Laboratories, Hanscom Air Force Base, Massachusetts, July 1974.

2. H.C. Merchant, E.M. Hernandez and N.D. McMullen, "Stabilized Laser Gravimeter," Proceedings of the 20th International Instrumentations Symposium, Albuquerque, New Mexico, May 1974.

3. J. Levine and J.L. Hall, "Design and Operation of a Methane Absorption Stabilized Laser Strainmeter," Journal of Geophysical Research, Vol. 77, No. 14 (May 1972) pp. 2595-2609.

4. L. Meirovitch, Analytical Methods in Vibrations, Macmillan, New York (1967).

5. H. Lurie, "Lateral Vibrations as Related to Structural Stability," Journal of Applied Physics, June 1952, pp. 195-204.

6. Laser Stabilized Gravimeter Quarterly Report, Nos. 3 through 7, Contract F19628-75-C-0042 (1975-76).

7. H. Barrell and J.E. Sears, "The Refraction and Dispersion of Air for the Visible Spectrum," Philosophical Transactions of the Royal Society of London, Series 4, Vol. 238 (1940) pp. 1-64.

8. Elden Bengt, "The Dispersion of Standard Air," Journal of the Optical Society of America, Vol. 43, No. 5 (May 1, 1953), pp. 339-344.

9. Elden Bengt, "The Refractive Index of Air," Metrologia, Vol. 2, No. 2 (April 1966) pp. 71-80.

10. James C. Owens, "Optical Refractive Index of Air: Dependence on Pressure, Temperature and Composition," Applied Optics, Vol. 6, No. 1 (January 1967) pp. 51-59.

11. N.D. McMullen, "Methane Absorption Stabilized Laser Gravimeter: Design of an Ultra-Sensitivity Fabry-Perot Interferometer Accelerometer," M.S. Thesis, Mechanical Engineering, University of Washington, 1974.

12. L. Finnie and W.R. Heller, Creep of Engineering Materials, McGraw-Hill, New York, New York 1959.

13. G. Bondor, "Calibration and Error Analysis of a Stabilized Laser Gravimeter," M.S. Thesis, Mechanical Engineering, University of Washington (in preparation), 1977.

14. K. Eisinger, "Parametric Excitation of a Clamped Beam," Ph.D. Thesis, Mechanical Engineering, Univeristy of Washington (in preparation), 1977.

15. P.W. Rodgers, "Parametric Phenomena as Applied to Vibration Isolation and Mechanical Amplifiers," Journ. Sound and Vib., Vol. 5, No. 3 (1967) p. 486.

16. P.W. Rodgers, "Sub-Resonant Response of a Mechanical System, Parametrically Excited at the Resonant Frequency," Nature, August 21, 1965, p 853.

17. P.W. Rodgers, "A Spring with Time-Variable Stiffness," Journ. of Acoust. Soc. of Am., Vol. 39, No. 4 (1966) p. 749.

18. P.W. Rodgers, "A Phase Sensitive Parametric Seismometer," Bull. of Seismological Soc. of Am., Vol. 56, No. 4 (1966) p. 949.

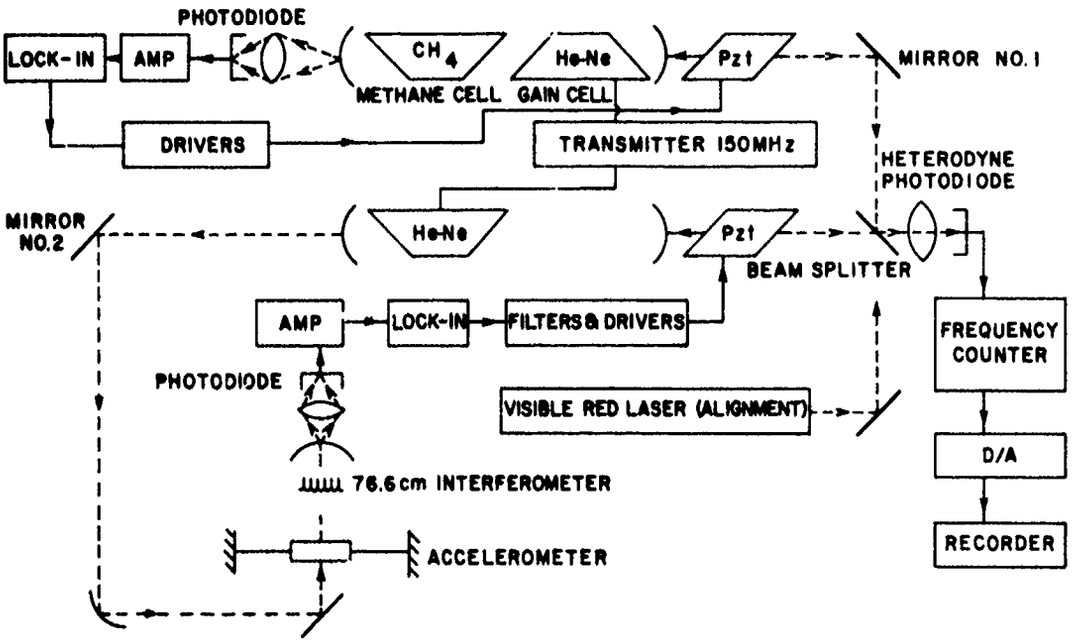

Figure 1. System schematic.

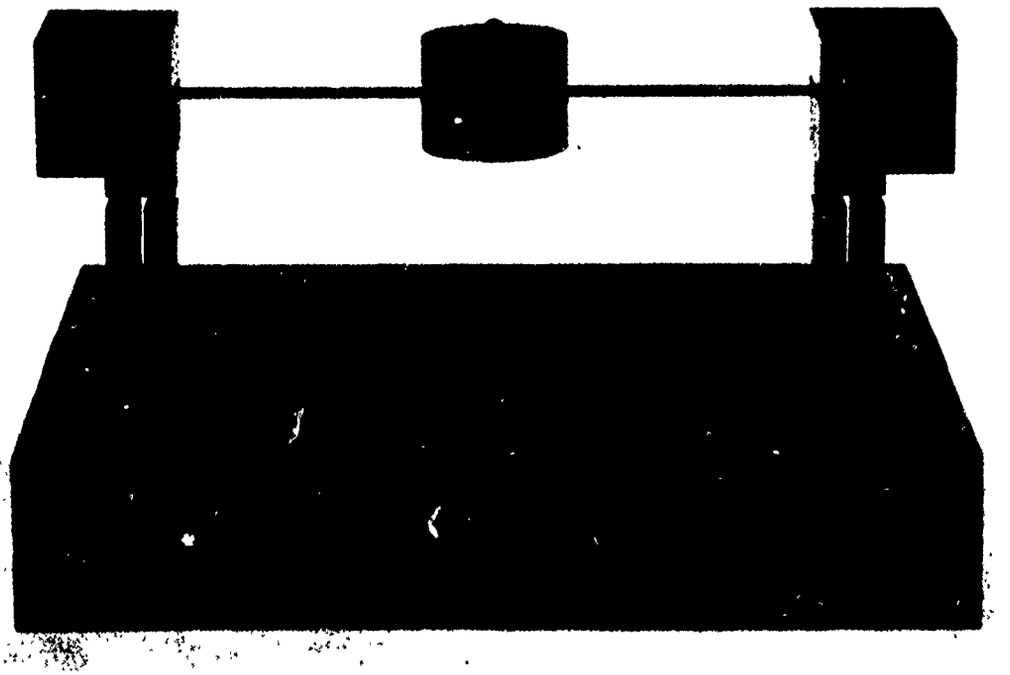

Figure 2. Mechanical sensor support system.

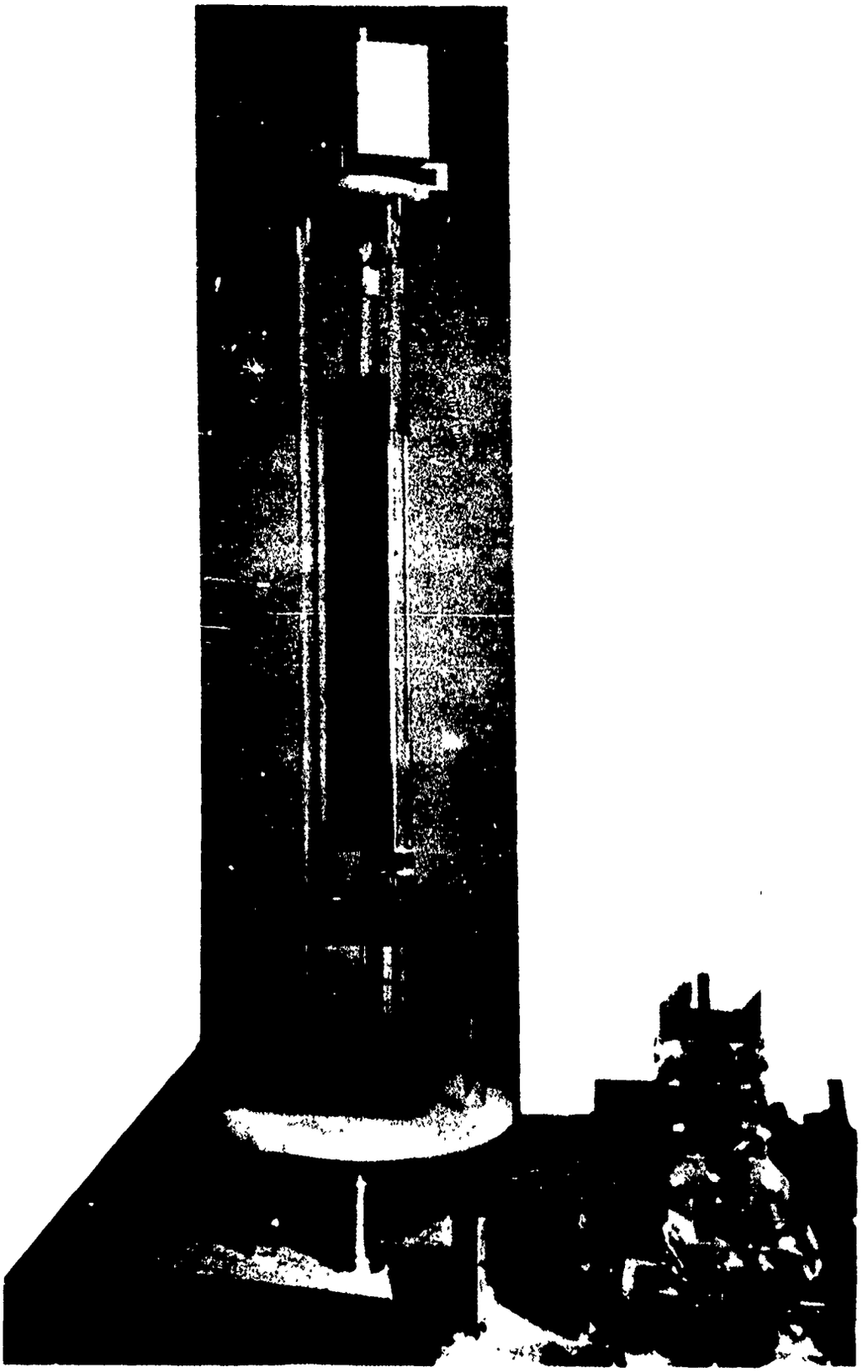

Figure 3. Fabry-Perot sensing cavity.

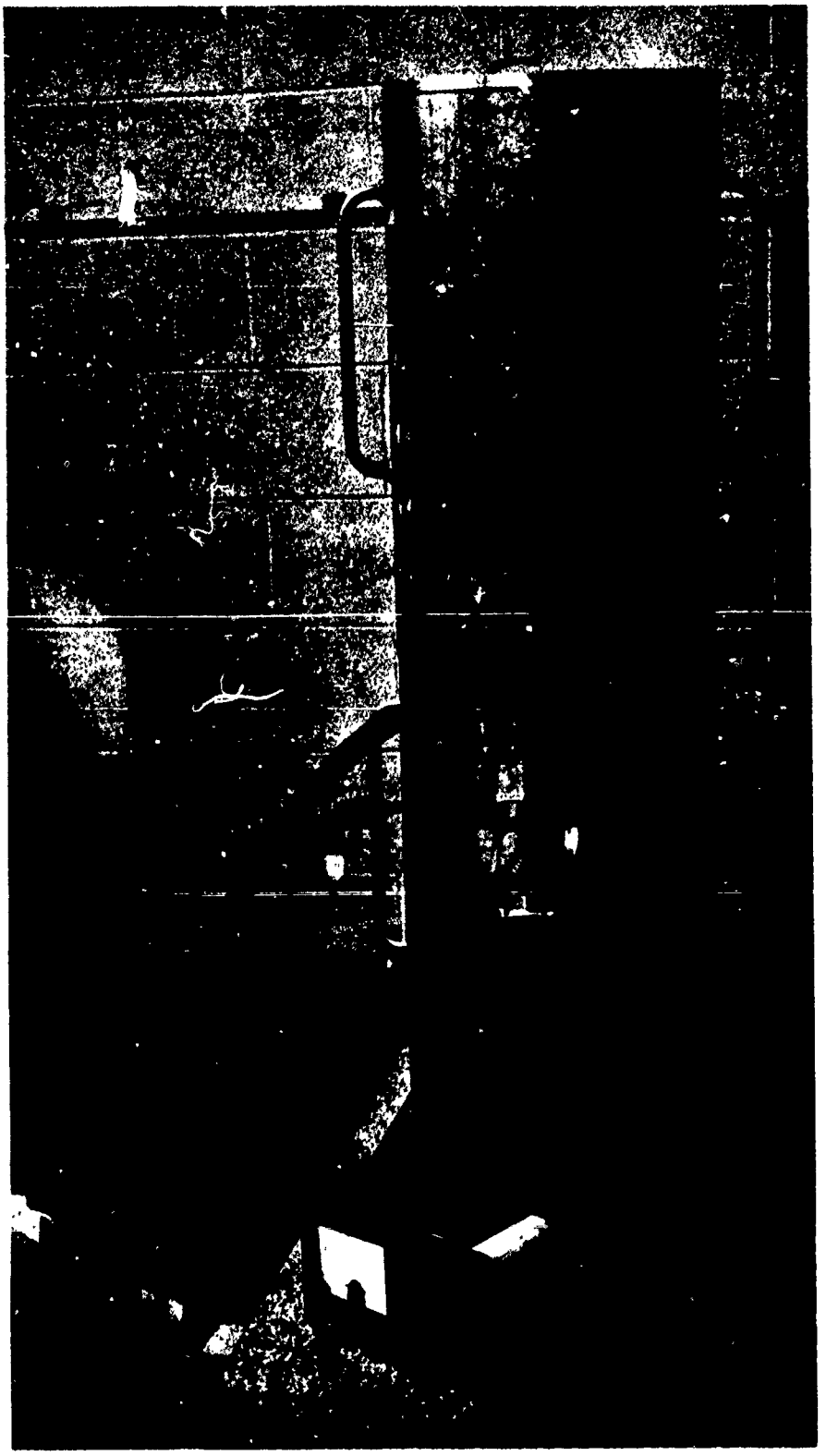

Figure 4. Cavity vacuum chamber

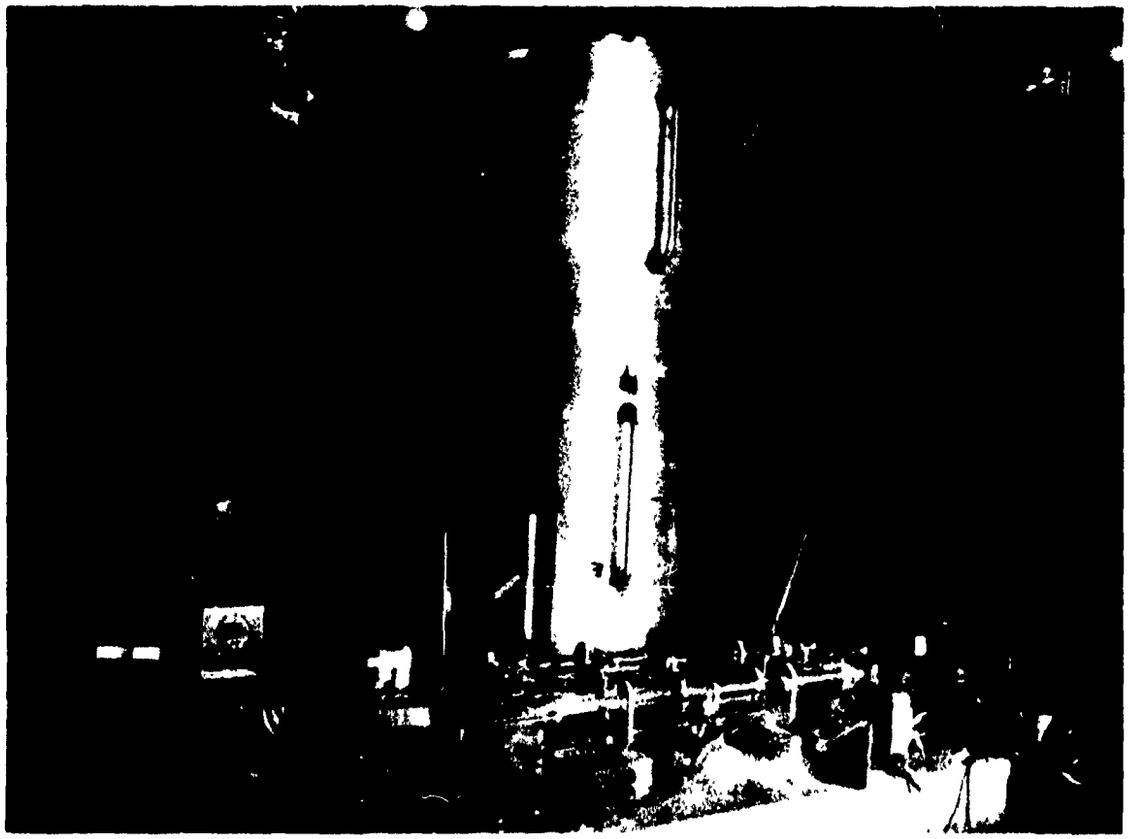

Figure 5. Field system.

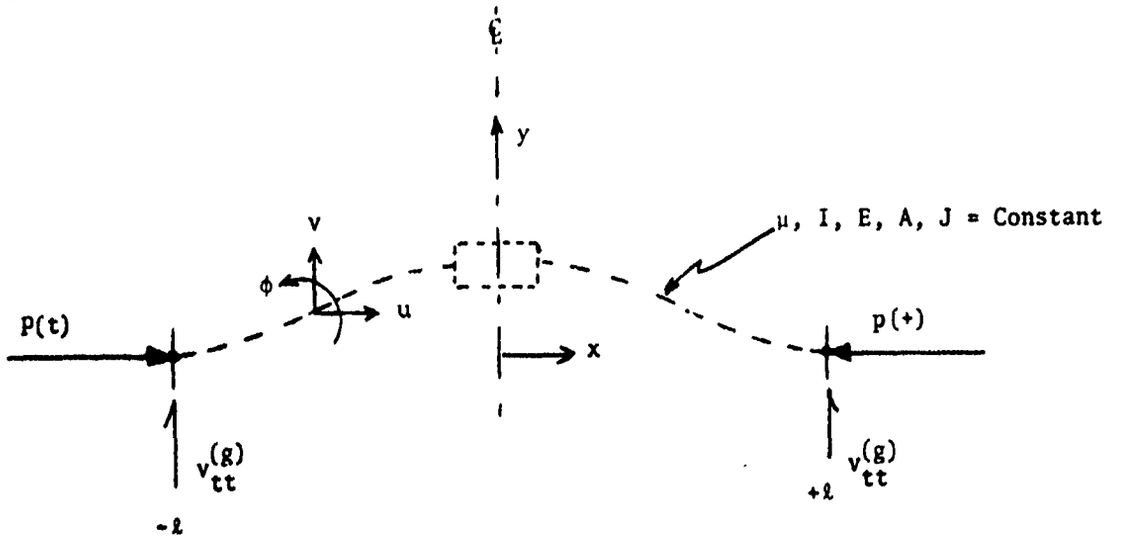

Figure 6. Schematic of mechanical sensor.

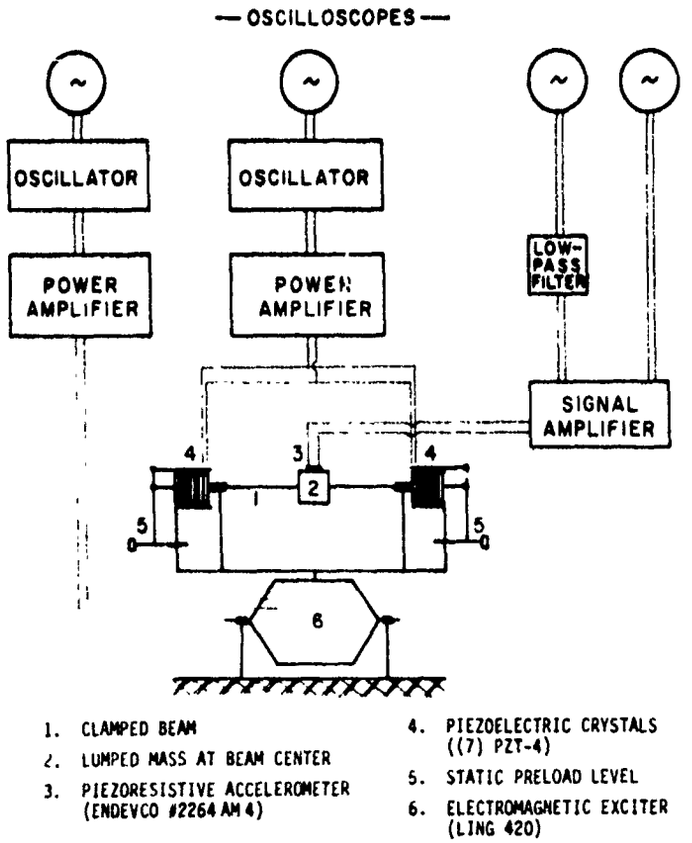

Figure 7. Schematic of test setup.

Figure 8. Parametric excitation sensor model.

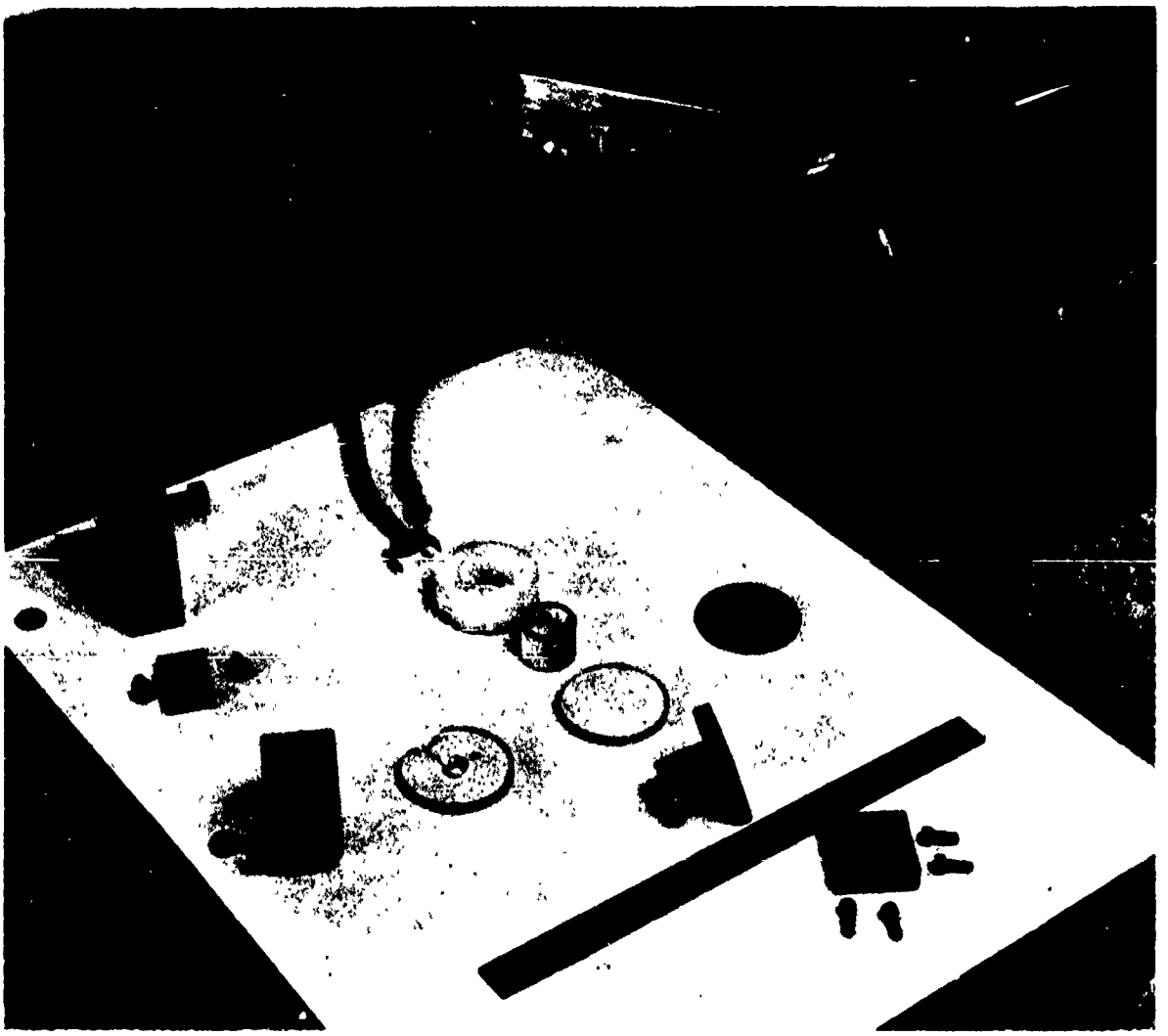

Figure 9. Excitation system components.

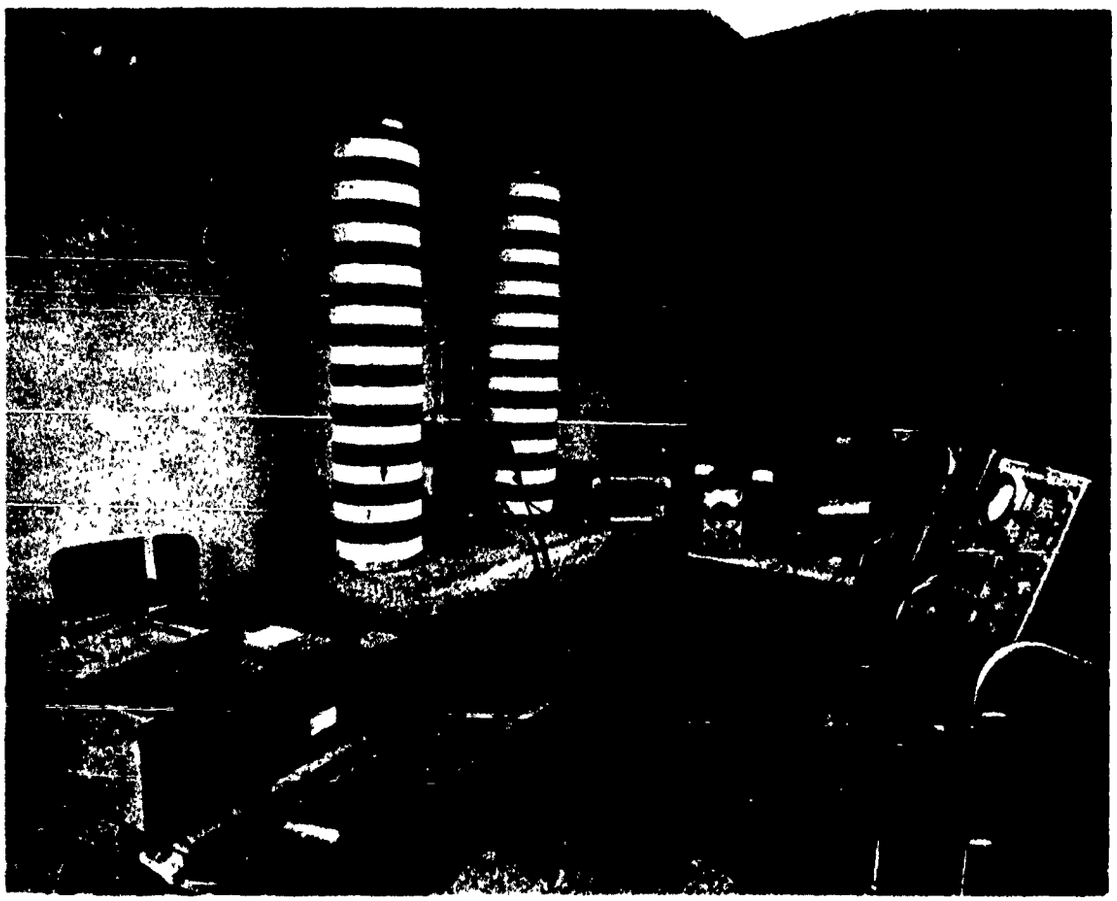

Figure 10. Parametric excitation system.

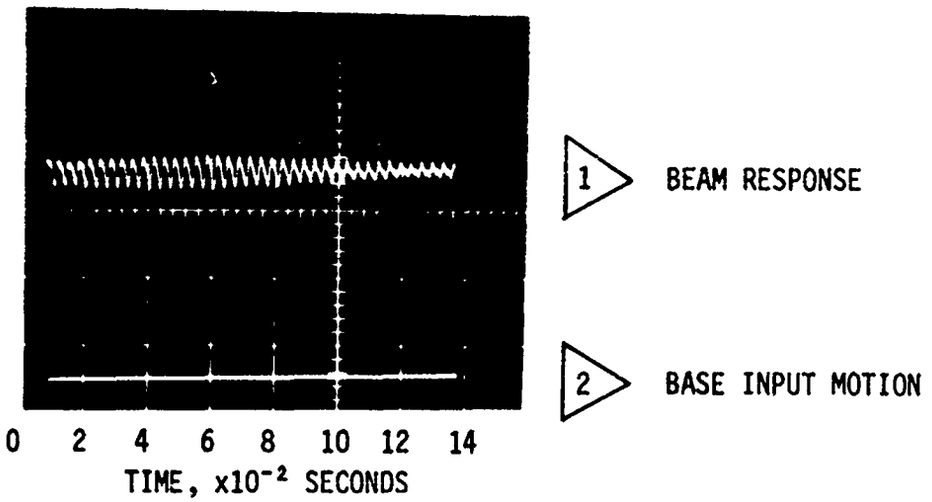

A. ENDLOAD FREQUENCY = 2 x SYSTEM'S NATURAL FREQUENCY; NO BASE MOTION

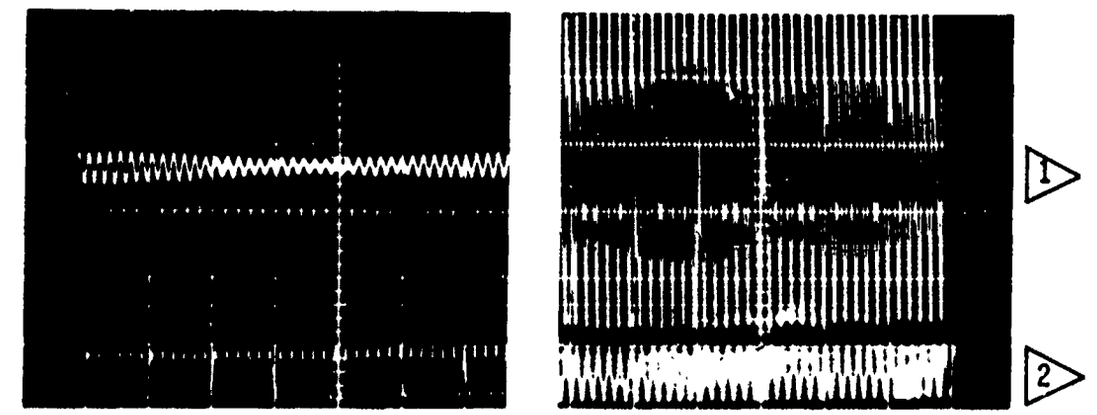

B. NO DYNAMIC END LOAD; NOMINAL BASE MOTION

C. ENDLOAD FREQUENCY = 2 x SYSTEM'S NATURAL FREQUENCY; NOMINAL BASE MOTION INPUT; PHASE LOCKED

Figure 11. Primary parametric amplification phenomenon, clamped-clamped.

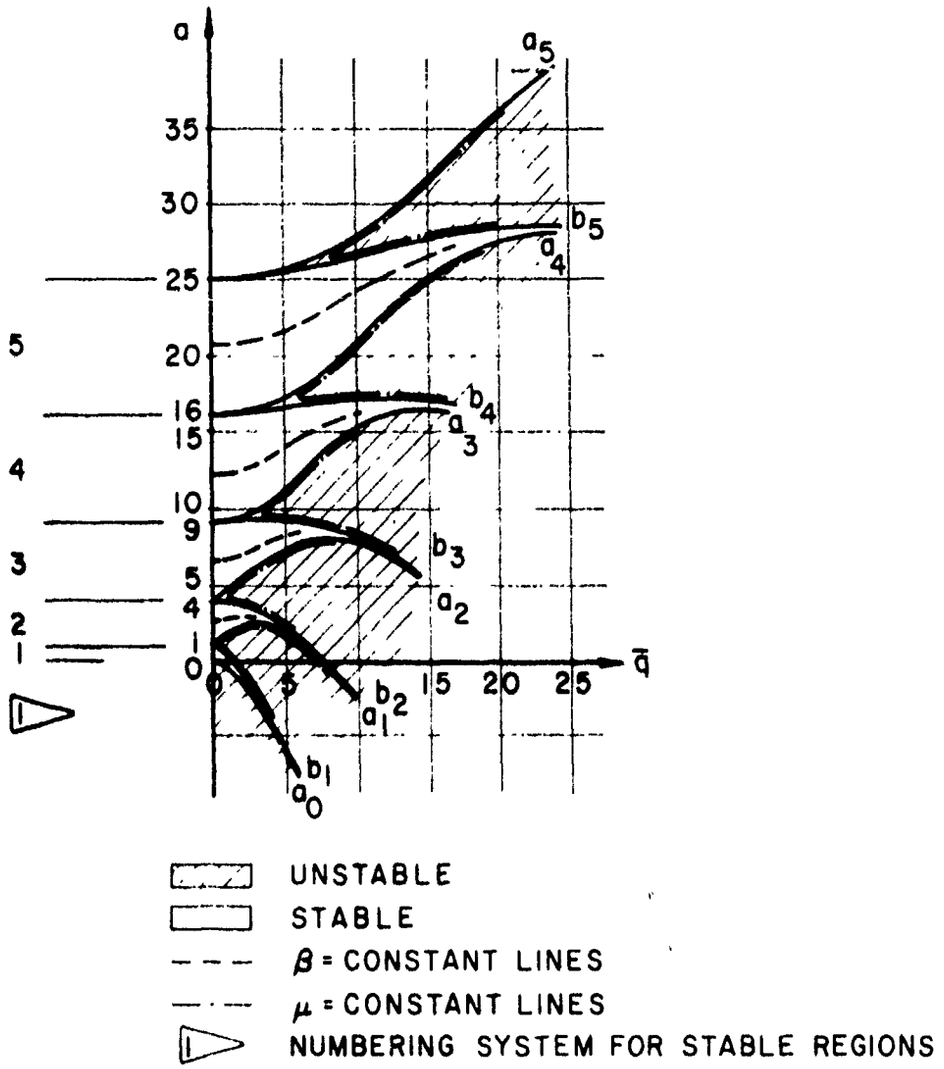

Figure 12. Mathieu equation stability.

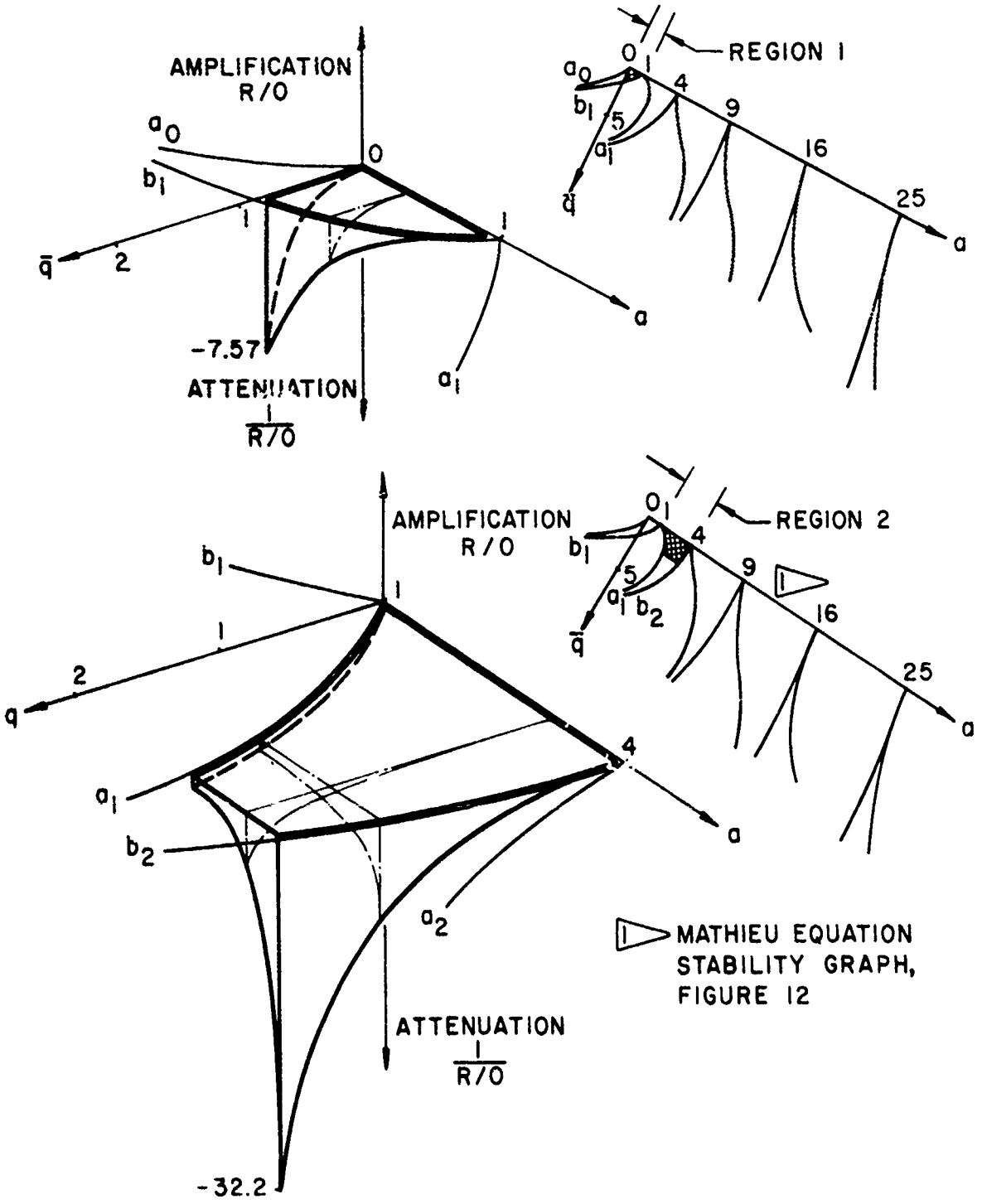

Figure 13. Secondary parametric amplification; characteristic regions 1 (top) and 2 (bottom) of Figure 12.

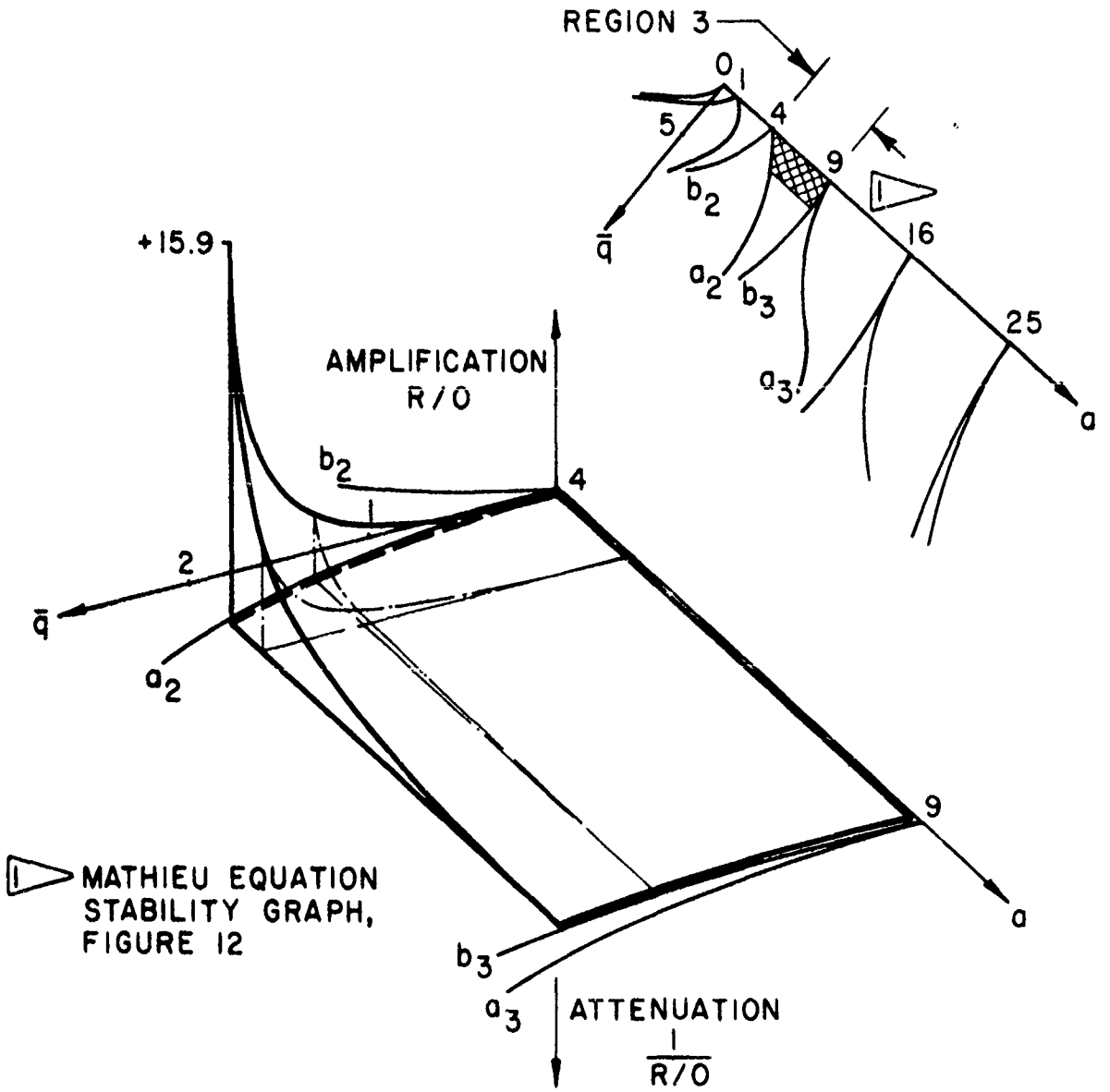

Figure 14. Secondary parametric amplification; characteristic region 3, Figure 12.

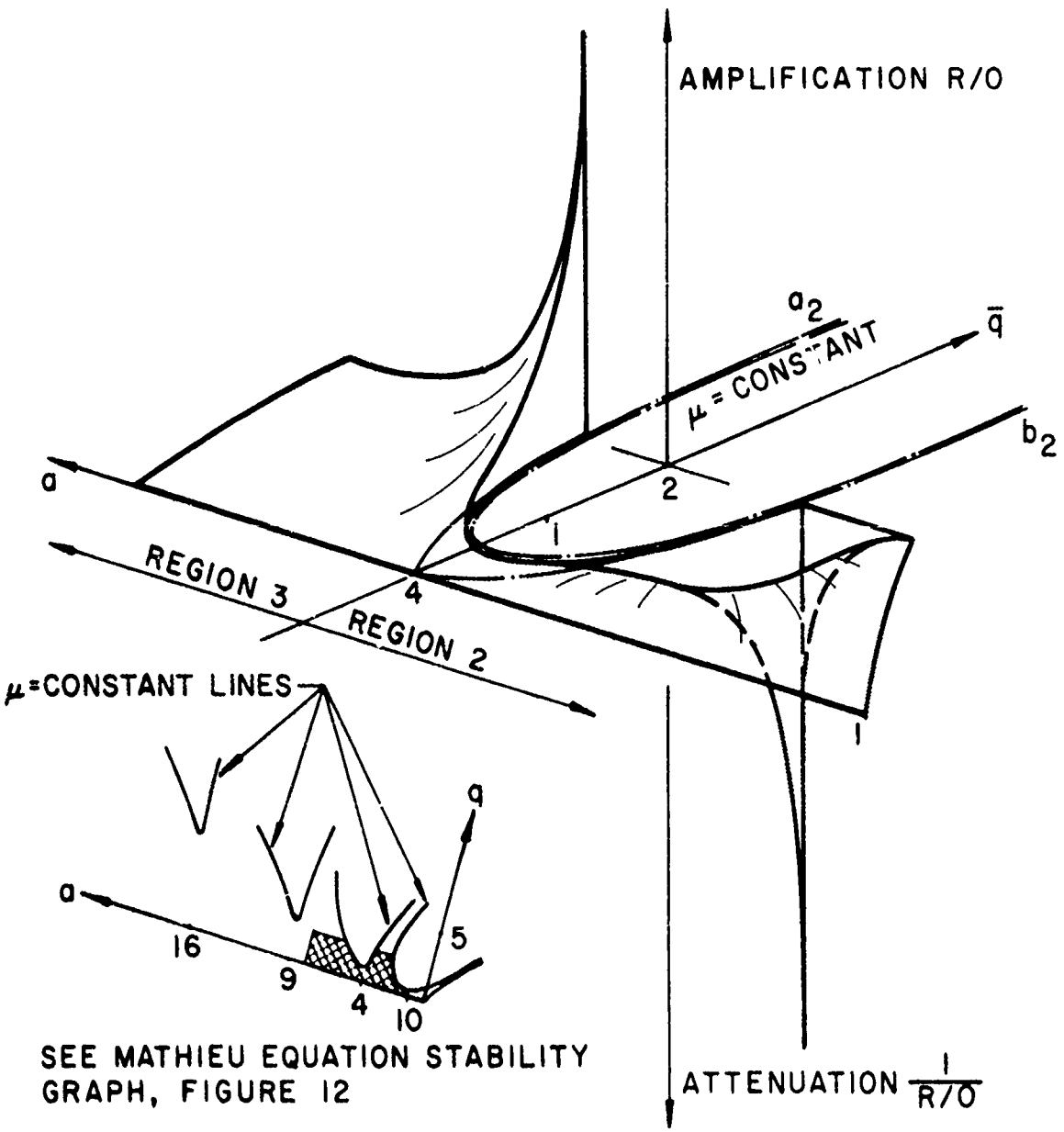

Figure 15. Secondary parametric amplification with damping.

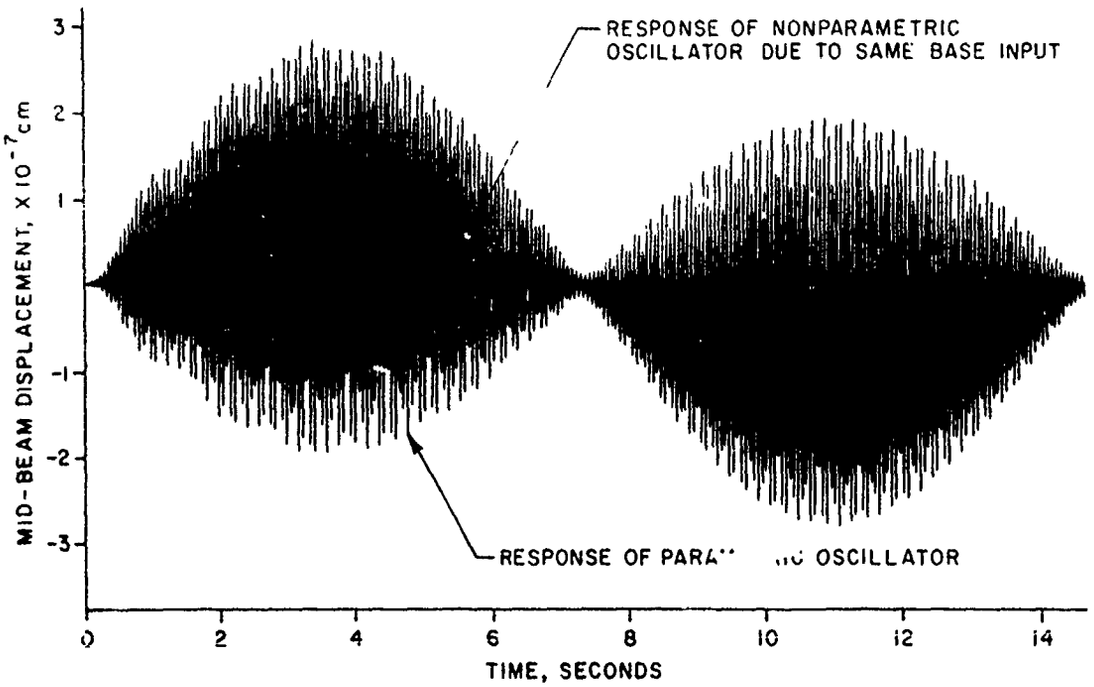

Figure 16. Numerical analysis of a clamped straight beam.

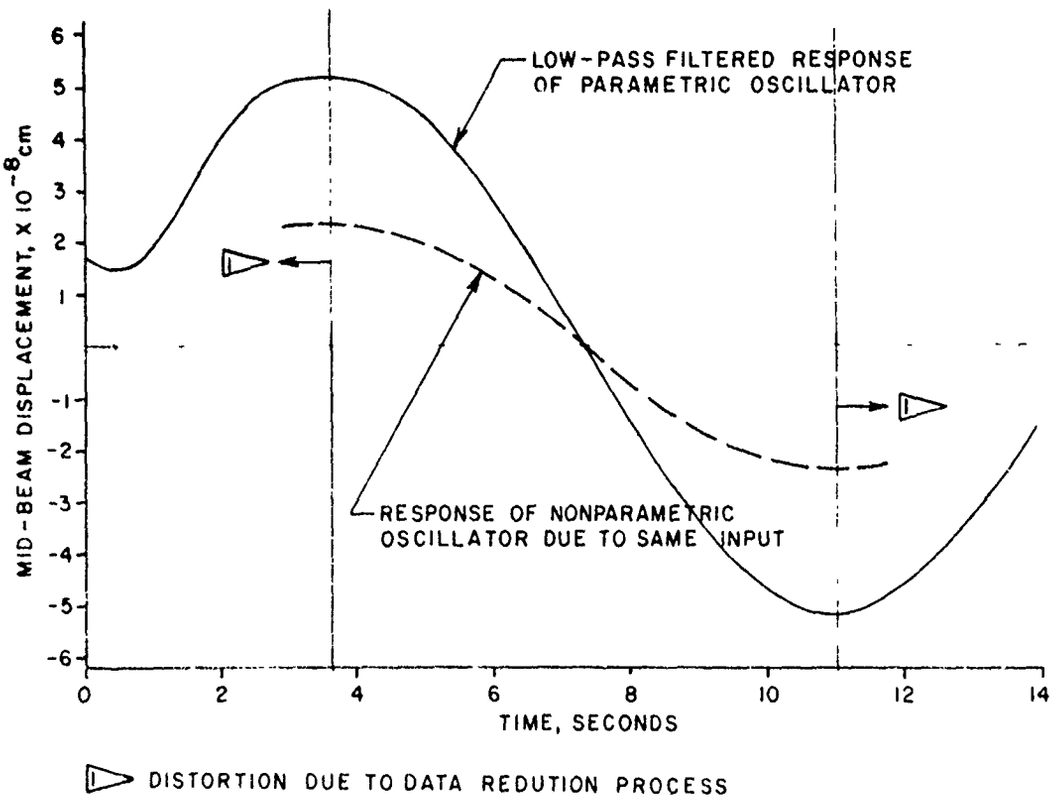

Figure 17. Low-pass filtered response of a clamped-clamped beam.

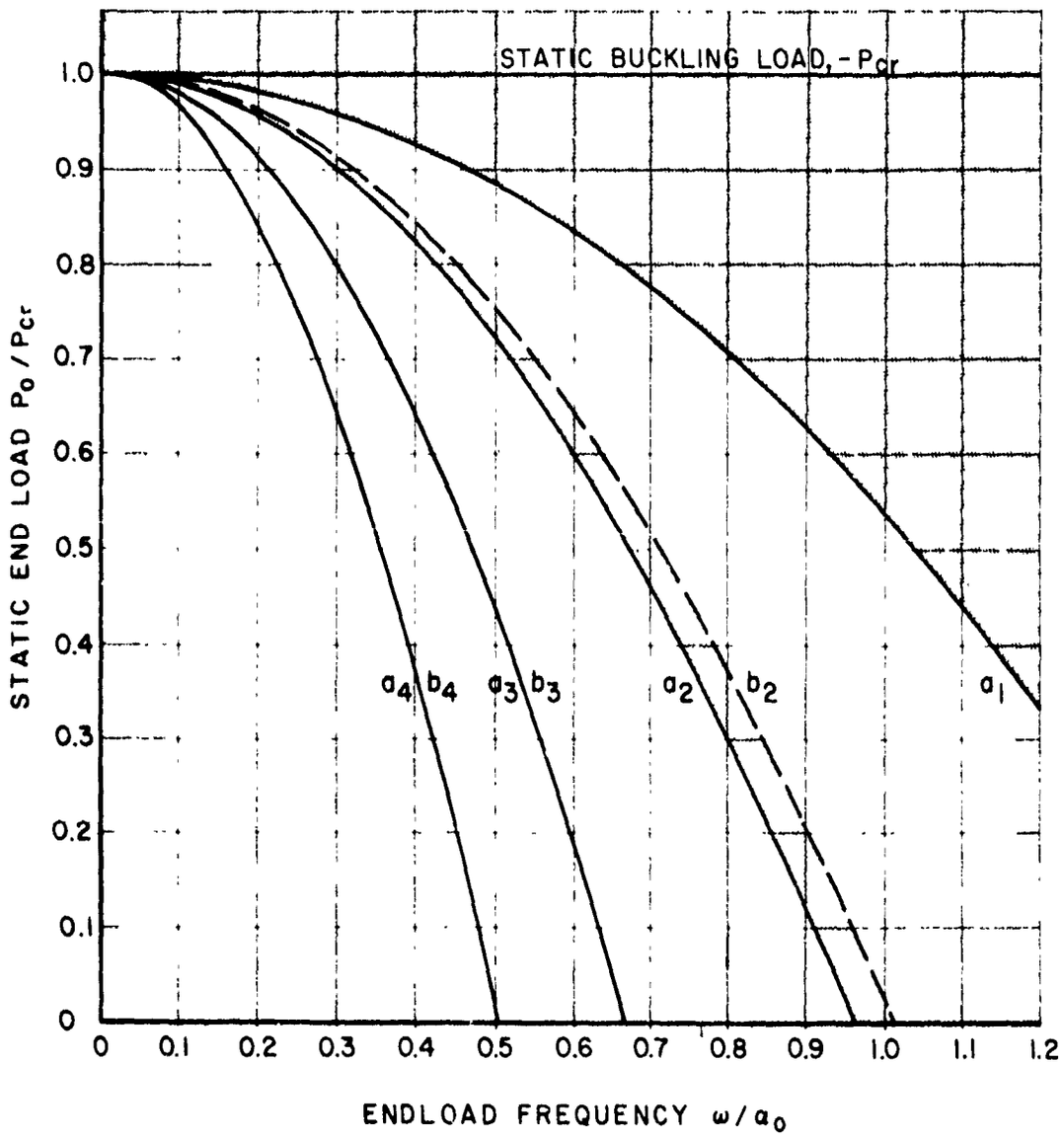

Figure 18. Interaction of system parameters a, $\bar{q}$, P_o and ω for $\bar{q}$ = 1.0, Figure 12.

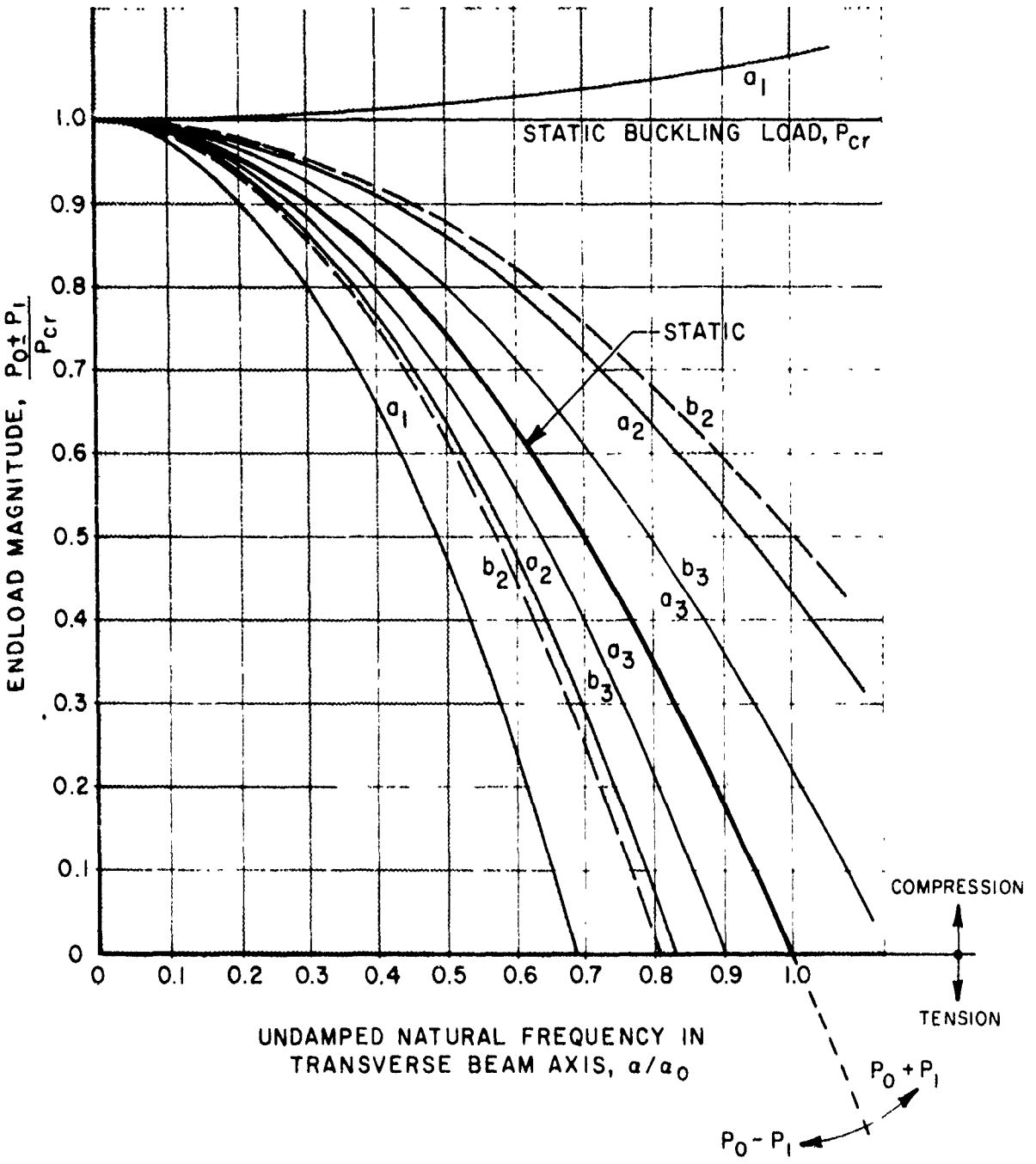

Figure 19. Interaction of system parameters a, $\bar{q}$, P_0, P_1 and α for $\bar{q}$ = 1.0, Figure 12.

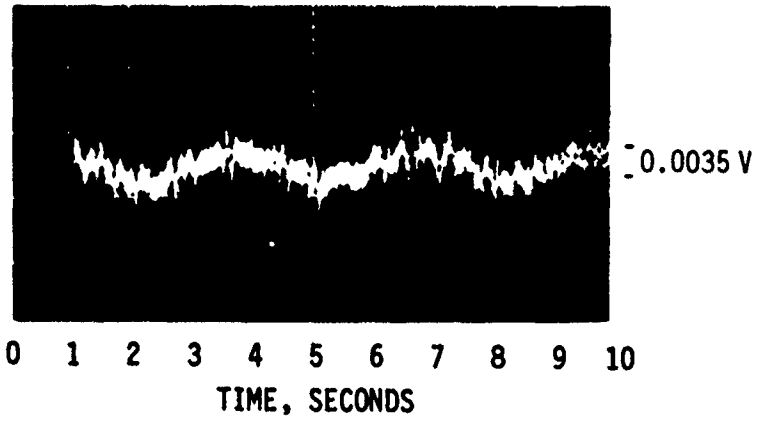

(a) NO DYNAMIC END LOAD

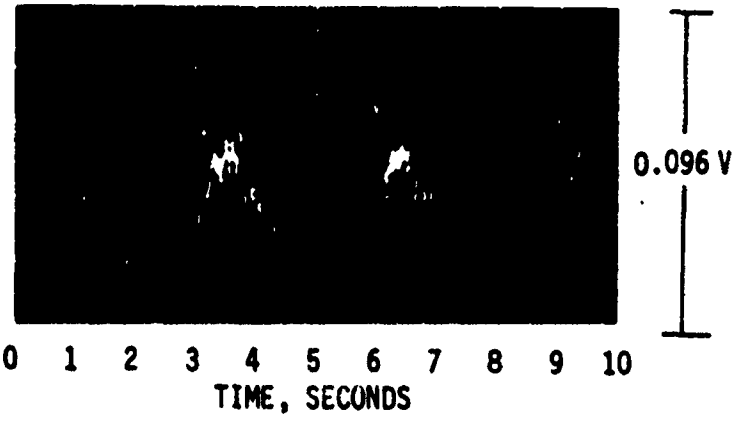

(b) DYNAMIC END LOAD

SYSTEM'S NATURAL FREQUENCY = 9 Hz
ENDLOAD FREQUENCY = 8.7 Hz
AMPLITUDE = 2.2×10^5 DYNES
BASE FREQUENCY = 0.33 Hz

Figure 20. Secondary parametric amplification phenomenon for a clamped-clamped beam.

APPENDIX A

BACKGROUND AND LITERATURE SURVEY, PARAMETRIC EXCITATION

The phenomenon of parametric excitation of oscillatory systems has been known for many years. The literature describing and evaluating this phenomenon goes back to the nineteenth century. In 1831 M. Faraday [1] observed parametrically induced oscillations on vibrating surfaces. Later, similar discoveries were made and reported by F. Melde in 1859 [2] and by Lord Rayleigh in 1883 [3]. The mathematics to allow analytical treatment of the classical problems was developed simultaneously by Mathieu in 1868 [4] and Hill in 1886 [5]. Thus the phenomenon of parametric excitation was first discovered on mechanical systems. Years later, however, these effects were studied and applied effectively to electrical circuits by Brillouin in 1897 [6] and by Poincaré in 1907 [7]. In the years to follow, the phenomenon of parametric excitation of oscillatory systems has found an ever increasing number of applications, many of which are in the field of electronic circuit theory.

Investigations of transverse vibrations of uniform beams have been conducted since the beginning of this century. Early investigators were mainly concerned with the general form of the governing differential equation of motion for free transverse vibration of uniform beams for various end conditions. Second-order corrections, such as terms for transverse shear, rotary inertia, damping, etc., were also proposed. Most of this early work can be found in papers by Holzer [8], Timoshenko [9], Muto [10], Sezawa [11], and Suyehiro [12]. The best known result of these studies is the familiar Timoshenko Beam Equation, which includes both transverse shear and rotary inertia of the differential beam section (see also [31]). The effects of compressive end loads on a slender column, in particular on its frequency behavior, were initially studied by Sezawa [13, 14], Howland [15], Cowley [16], and Levy [17].

More recent investigators of transverse vibrations of uniform beams are again concerned with second-order nonlinearities in the beam equation. In general, such nonlinearities arise from:

a) longitudinal constraints which are either movable or immovable

b) some initial curvature of the beam

c) inclusion of transverse shear

d) rotational inertia terms

e) longitudinal inertia terms.

Some analyses that focus primarily on the nonlinear elasticity terms, such as a) to c), were published by Eringen [18], Woinowski-Krieger [19], McDonald and Raleigh [2], Burgreen [21], Wahi [22], Eisley [23], Bennett and Eisley [24], Tseng and Dugundji [25, 26], Srinivasan [27] and Lurie [28]. The resulting equations of motion obtained by the above authors

are restricted to vibration amplitudes that are less than or equal to the thickness of the beam as well as to fixed end coordinates (as compared to constant end loads). Solutions to these equations have been obtained as follows: by Eringen [18] by means of perturbation techniques; by McDonald and Raleigh [20] using an expansion into Jacobian elliptic functions of time; by Burgreen [21] by assuming a starting mode shape and solution of the resulting integral equation of motion using elliptic integral representation of time; by Bennett and Eisley [24] using the forced response in a three-mode case; by Tseng and Dugundji [25, 26] using Galerkin's method and a solution of the resulting Duffing equation by the harmonic balance method; and by Srinivasan [27] using the Ritz averaging method in both space and time variables to study the steady state forced response in two modes. The papers of Tseng and Dugundji are of particular interest since in addition to simple harmonic motion they address sub- and superharmonic motion. Other papers that also address this subject were published by Snowdon [34, 35] and Sridhar, Nayfeh and Mook [36]. Using the Timoshenko Beam Equation, which considers transverse shear and rotary inertia terms non-negligible, Snowdon computes displacement amplification curves for various end conditions of free vibration in his first paper [34] and of forced vibration in his second paper [35]. The paper by Sridhar, Nayfeh and Mook [36] departs from a general second order nonlinear equation into which the nonlinear beam equation always can be cast and presents solutions using perturbation techniques, i.e., the method of multiple scales as developed by Nayfeh (see [58]) and other authors. Subharmonics, superharmonics and combination resonances are investigated; the study considers a multiple degree of freedom system.

In contrast to the papers mentioned previously, in which primarily "elastic nonlinearities" are considered, Atluri [29] addresses the problem of modification of the equation of motion by inclusion of longitudinal and rotational inertia terms only. Using Galerkin's method to derive the equations of motion, he finds solutions to these equations by means of perturbation techniques.

Another kind of continuous beam problem is the one of constant end loads as compared to constant end coordinates which was considered above. Such problems have been discussed extensively by Lord Rayleigh [30] and Timoshenko [31]. While all previous references are restricted to amplitudes of oscillation that do not exceed the thickness of the beam, a paper by Woodall [32] addresses large amplitude oscillations of thin elastic beams. The solutions to his equations of motion--which he derives by means of the Galerkin method--use the perturbation method and the finite difference method. The influence of a concentrated mass on the free vibration of a uniform beam is discussed in a paper by Maltbaek [33]. Starting with a sixth-order frequency determinant, his paper lists expressions for the beam frequencies according to end conditions and location of the concentrated mass.

Another class of literature is the one that describes the application of the phenomenon of parametric excitation to certain mechanical systems. As noted previously, parametric amplifiers have (although they were discovered in mechanical systems) found in recent years increasingly more

applications in electrical engineering. Some of the more recent classical references in this field are by Blackwell and Kotzebue [37] and Tucker [38]. Application of the parametric phenomenon to mechanical oscillatory systems often leads to the classical problem of the dynamic stability of slender columns that are subjected to periodic longitudinal forces. The basic concern that led to most studies in this area is the occurrence of excitation of the fundamental transverse beam frequency at longitudinal forcing frequencies other than the fundamental frequency. This presents a serious design problem, in particular, for some aircraft structures. Two of the early authors on this subject were Utida and Sezawa [39]. In their report, the authors discuss extensive testing of a brass cantilever beam with a concentrated mass at its end; the periodic end load was applied through a magnetic field at the free end. The mathematical treatment of the problem was limited to stability investigations of the well known Mathieu equation into which the problem was cast. It is interesting to note that the authors found that instabilities of the system (or conversely parametric excitation) occur at ratios of the natural transverse beam frequency of 1/2, 2/2, 3/2, 4/2, 5/2,..., with a decrease of the resonant amplitude with increase of this ratio. Similar results have been found by many authors to follow.

A somewhat different analytical approach to this problem was taken by Mettler [40, 41, 42]. In his works, Mettler used energy principles, in particular the principle of virtual displacement (see also Marguerre [43]) and Hamilton's Principle to derive the equations of motion of a pinned, uniform, homogeneous beam under periodic axial loading. In his papers, Mettler reduces the equations of motion to a system of n homogeneous, linear, second-order differential equations with periodic coefficients in the form of a general Mathieu equation which he solves with a so-called double series development. One is a trigonometric series and the other a perturbation series. He obtains plots of instability regions that are similar to those obtained by Utida and Sezawa [39] but they are developed by purely analytical methods. These papers are particularly noteworthy since they depart from the basic principles of the theory of elasticity to derive the required energy relations. Investigations based on these fundamental papers were published by Mettler and Weidenhammer [44] and Weidenhammer [45, 46, 47]. An interesting finding reported in the paper by Mettler and Weidenhammer [44] is, that if a beam is subjected to harmonic end coordinate displacements the spring behavior is of the hardening type; if the beam is subjected to harmonic end loads only, it essentially behaves linearly with theoretically unlimited growth of amplitude (neglecting second-order nonlinearities in the equation). If a concentrated mass is located at one end and the beam is subjected to harmonic end loads, the spring behavior is of the softening type. These analyses address a pinned configuration. A paper by Weidenhammer [45] studies the problem of a clamped beam configuration with a periodic axial force. The treatment of this problem is much like that of the pinned problems by Mettler [40, 41, 42] and in fact is based upon the same theoretical aspects.

Another analysis approach to problems on flutter and autoparametric resonances is taken by Herrmann and Hauger [48] by presenting solutions in the form of Fourier series. The special problem of "snap-through"

(symmetrical) and one-sided (unsymmetrical) vibrations of columns is presented in a paper by Min and Eisley [49]. Based on a paper by Wahi [22] that assumes the space and time variables are separable, the authors use a normal mode solution in the form of an assumed series. Limiting the discussion to the assumption of two modes, the authors find an approximate solution to the nonlinear equation of motion using the harmonic balance method. Analog computer solutions are also used for comparison with the analytical results.

Finally, a series of papers was written by Rodgers [50, 51, 52, 53] on the development of a mechanical parametric amplifier and its application as a phase sensitive parametric seismometer. In contrast to the previous references, these papers discuss the general behavior that is to be expected of a damped single degree of freedom oscillator with a spring of time-variable stiffness [52]. The spring used by Rodgers [52] is of the magneto-mechanical type. A noteworthy aspect of this paper is a clear demonstration of the phase sensitivity of the ratio of the input to the parametric response, e.g., the amplification curve. Only primary effects at endload frequencies of twice the oscillator natural frequency and of the natural frequency and no nonlinearities are considered.

Besides the above papers, a series of reference texts have appeared that address chapters to the phenomena of parametric amplification of oscillatory motion. The references of interest, which are by Minorsky [54], Bolotin [55], and Kononenko [56], were all originally Russian publications.

Information on the type of data that is to be measured by a gravimeter, which is the proposed application of this device, is given in a text on earth tides by Melchior [57].

Bibliography

1. M. FARADAY, "On a Particular Class of Acoustical Figures, and on Certain Forms Assumed by a Group of Particles....," Phil. Trans. Roy. Soc., No. 121 (1831), p. 299.

2. F. MELDE, "Über die Erregung stehender Wellen eines fadenförmigen Körpers," Ann. der Physik u. Chemie, Ser. 2-109 (1859), p. 193.

3. LORD RAYLEIGH, "On the Crispation of Fluid Resting Upon a Vibrating Support," Phil. Mag., No. 16 (1883), p. 50.

4. E. MATHIEU, "Mémoire sur le mouvement vibratoire d'une membrane de forme elliptique," Jour. de Mathe. Pure et Appliquées, No. 13 (1968), p. 137.

5. G.W. HILL, "Mean Motion of the Lunar Perigee," Acta Math., No. 8 (1886).

6. L. BRILLOUIN, Eclairage Electrique, April 1897.

7. H. POINCARÉ, Eclairage Electrique, March 1907.

8. H. HOLZER, "Biegeschwingungen mit Berücksichtigung der Stabmasse und der äusseren und inneren Dämpfung," Zeitschr. f. angew. Math. und Mech., Bd. 8, Heft 4 (1928), pp. 272-283.

9. S. TIMOSHENKO, Phil. Mag., Ser. 6, Vol. 41, p. 744 and Phil. Mag., Ser. 6, Vol. 43, p. 135.

10. K. MUTO, Zeitschr. f. angewand. Math. und Mech., Bd. 10 (1930), p. 346.

11. K. SEZAWA, Bull. Earthqu. Res. Inst., Tokyo, Vol. 3 (1927), p. 50.

12. K. SUYEHIRO, Proc. Imp. Acad., Vol. 4 (1928), p. 263 and Bull. Earthqu. Res. Inst., Tokyo, Vol. 6 (1929), p. 63.

13. W.L. COWLEY and H. LEVY, Proc. Roy. Soc., London, Vol. 95 (1919), p. 440.

14. R.C.J. HOWLAND, Phil. Mag. 7, Vol. 1 (1926), p. 674.

15. K. SEZAWA, Jour. Aeron. Res. Inst., Tokyo, No. 5 (1924), p. 39.

16. K. SEZAWA, Rep. Aeron. Res. Inst., Tokyo, Vol. 4, No. 45 (1928), p. 107.

17. K. SEZAWA, "Die Wirkung des Enddruckes auf die Biegeschwingung eines Stabes mit innerer Dämpfung," Zeitschr. f. angewand. Math. und Mech., Bd. 12, Heft 5 (1932), p. 275.

18. A.C. ERINGEN, "On the Nonlinear Vibrations of Elastic Beams," Quart. of Appl. Math., Vol. 9 (1952), p. 361.

34. J.C. SNOWDON, "Transverse Vibration of Simply Clamped Beams," Jour. of Acoust. Soc. of Am., Vol. 35, No. 8 (1963), p. 1152.

35. J.C. SNOWDON, "Transverse Vibration of Beams with Internal Damping, Rotary Inertia and Shear," Jour. of Acoust. Soc. of Am., Vol. 35, No. 12 (1963), p. 1997.

36. S. SRIDHAR, A.H. NAYFEH and D.T. MOOK, "Nonlinear Resonances in a Class of Multi-Degree of Freedom Systems," Jour. of Acoust. Soc. of Am., Vol. 58, No. 1 (1975), p. 113.

37. L.A. BLACKWELL and K.L. KOTZEBUE, Semiconductor-Diode Parametric Amplifier, Prentice-Hall, Inc., Englewood Cliffs, N.J. (1961).

38. D.G. TUCKER, Circuits with Periodically Varying Parameters, McDonald, London (1964).

39. I. UTIDA and K. SEZAWA, "Dynamical Stability of a Column under Periodic Longitudinal Forces," Rep. Aeron. Res. Inst., Tokyo Imp. University 15 (1940), p. 139.

40. E. METTLER, "Über die Stabilität erzwungener Schwingungen elastischer Körper," Ingenieur Archiv., Bd. 13 (1942), p. 97.

41. E. METTLER, "Eine Theorie der Stabilität der elastischen Bewegung," Ingenieur Archiv, Bd. 16 (1947), p. 135.

42. E. METTLER, "Allgemeine Theorie der Stabilität erzwungener Schwingungen elastischer Körper," Ingenieur Archiv, Bd. 17 (1949), p. 418.

43. K. MARGUERRE, "Über die Behandlung von Stabilitätproblemen mit Hilfe der energetischen Methode," Zeitschr. angew. Math. Mech., Bd. 18, Heft 1 (1938), p. 57.

44. E. METTLER and F. WEIDENHAMMER, "Der axial pulsierend belastete Stab mit Endmasse," Zeitschr. angew. Math. Mech., Bd. 36, Nr. 718 (1954), p. 284.

45. F. WEIDENHAMMER, "Der eingespannte, achsial pulsieren belastete Stab als Stabilitäsproblem," Ingenieur Archiv, Bd. 19 (1951), p. 162.

46. F. WEIDENHAMMER, "Stabquerschwingungen schwach vorgekrümmter Stäbe mit pulsierender Achslast," Zeitschr. angew. Math. Mech., Bd. 36, Nr. 5/6 (1956), p. 235.

47. F. WEIDENHAMMER, "Nichtlineare Biegeschwingungen des axial pulsierend belasteten Stabes," Ingenieur Archiv, Bd. 20 (1952), p. 315.

48. G. HERRMANN and W. HAUGER, "On the Interrelation of Divergence, Flutter and Auto-Parametric Resonance," Ingenieur Archiv, Bd. 42 (1973), p. 81.

49. GWO-BAO MIN and J.G. EISLEY, "Nonlinear Vibrations of Buckled Beams," Journal of Engineering for Industry, May 1972, p. 637.

50. P.W. RODGERS, "Parametric Phenomena as Applied to Vibration Isolators and Mechanical Amplifiers," Jour. Sound and Vib., Vol. 5, No. 3 (1967), p. 489.

51. P.W. RODGERS, "Sub-Resonant Response of a Mechanical System, Parametrically Excited at its Resonant Frequency," Nature, August 21, 1965, p. 853.

52. P.W. RODGERS, "A Spring with Time-Variable Stiffness," Jour. of Acoust. Soc. of Am., Vol. 39, No. 4 (1966), p. 749.

53. P.W. RODGERS, "A Phase Sensitive Parametric Seismometer," Bull. of Seismolog. Soc. of Am., Vol. 56, No. 4 (1966), p. 947.

54. N. MINORSKY, Nonlinear Oscillations, D. van Nostrand Co., Inc., 1962.

55. V.V. BOLOTIN, The Dynamic Stability of Elastic Systems, Holden-Day Inc., London, 1964.

56. V.O. KONONENKO, Vibrating Systems with a Limited Power Supply, London ILIFFE Books Ltd., 1969.

57. P. MELCHIOR, The Earth Tides, Pergamon Press, 1966.

58. A. NAYFEH, Perturbation Methods, John Wiley & Sons, 1973.